

One-loop induced contributions to the rare decay of $A_0 \rightarrow h_0 h_0 \gamma$ in Two Higgs Doublet Models

Dzung Tri Tran^{a,b}, L. T. Hue^{c,d}, Thanh Huy Nguyen^{e,f}, Vo Quoc Phong^{e,f}, Khiem Hong Phan^{a,b}

^a*Institute of Fundamental and Applied Sciences, Duy Tan University, Ho Chi Minh City 70000, Vietnam*

^b*Faculty of Natural Sciences, Duy Tan University, Da Nang City 50000, Vietnam*

^c*Subatomic Physics Research Group, Science and Technology Advanced Institute, Van Lang University, Ho Chi Minh City, Vietnam*

^d*Faculty of Applied Technology, School of Technology, Van Lang University, Ho Chi Minh City, Vietnam*

^e*Department of Theoretical Physics, University of Science, Ho Chi Minh City 700000, Vietnam*

^f*Vietnam National University, Ho Chi Minh City 700000, Vietnam*

Abstract

The analytic expressions for one-loop contributions to the rare decay process $A_0 \rightarrow h_0 h_0 \gamma$ within the CP-conserving of Two Higgs Doublet Models are first reported in this paper. Analytic results are presented in term of scalar one-loop Passarino-Veltman functions following the standard output of the packages `LoopTools` and `Collier`. In this context, physical results for the computed process are easily generated by using one of these packages. The numerical checks are proposed to verify for the analytic results in this paper. The checks rely on the renormalization conditions that the decay amplitude must be the ultraviolet finiteness and infrared finiteness. The amplitude consisting of an external photon always obeys the Ward identity. This will be confirmed numerically in this article. In phenomenological results, the decay rates of $A_0 \rightarrow h_0 h_0 \gamma$ are evaluated at several points in the allowed regions of the parameter space. Furthermore, the differential decay widths with respect to the invariant mass of Higgs-pair in final states are studied.

Keywords: Higgs phenomenology, One-loop Feynman integrals, Analytic methods for Quantum Field Theory, Physics beyond the Standard Model, Physics at present and future colliders.

1. Introduction

After discovering the Standard-Model-like Higgs boson (SM-like Higgs) h_0 at the Large Hadron Collider (LHC) [1, 2], the standard model (SM) theory of particle physics is being well-established. In spite of the great SM's success in describing most of the experimental data, the structure of the scalar Higgs sector in the SM is still an unknown question. There is no theoretical principle for the minimum of scalar Higgs sector selection in the SM. In many physics beyond the SM (BSM), the Higgs potential is extended by adding new scalar singlets and/or multiplets. Subsequently, many additional scalar bosons appear, such as neutral CP-even, CP-odd, and charged Higgs bosons. In the context of experimental searches, the precise measurements for the decay widths and the production cross-sections for all the above-mentioned scalar particles could play important roles in exploring the Higgs sector, understanding deeply the origin of the electroweak symmetry breaking mechanism (EWSB) as well as probing new physics signals. Among the mentioned scalar particles, decay and processes of CP-odd (A_0) are of considerable interest. Recently, direct production of a light CP-odd Higgs boson has been performed at the

Email address: phanhongkhiem@duytan.edu.vn (Khiem Hong Phan)

Tevatron and LHC [3]. Searches for the decay $A_0 \rightarrow Zh_0$ in pp collisions have been carried out at the LHC [4]. Probing for a light pseudoscalar Higgs boson in $\mu\mu\tau\tau$ events at the LHC in Refs. [5, 6] and in the di-muon decay channels in pp collisions at $\sqrt{s} = 7$ TeV has been reported in Ref. [7].

In the aspects of theoretical studies, the detailed computations for one-loop and higher-loop corrections to the decay width of CP-odd Higgs boson are necessary for matching the higher-precision data at future colliders. One-loop corrections to two-body decay of CP-odd Higgs within the CP-conserving of the Two Higgs Doublet Models (THDM) have been performed in Refs. [8, 9, 10, 11]. One-loop analyses for the most important decay channel $A_0 \rightarrow Zh_0$ have been studied in Refs. [12, 13]. Furthermore, one-loop electroweak corrections to the decay of A_0 into a pair of scalar fermion have been calculated in Refs. [14, 15] within the context of minimal supersymmetric extension of the Standard Models (MSSM). The CP-odd Higgs decay rates to two gluons have been evaluated by applying the Pade improvement method in Ref. [16]. More recently, one-loop contributions to $A_0 \rightarrow \ell\bar{\ell}V$ with $V = \gamma, Z$ in the context of Higgs Extensions of the Standard Models like the THDM and Triple Higgs Models (THM), etc., have been computed in Ref. [17]. The CP-odd Higgs boson productions associated with a neutral Z boson at the LHC within the MSSM framework have been evaluated in Ref. [18]. Evaluating for the productions of CP-odd Higgs boson at future $e^- \gamma$ colliders has been considered in Ref. [19]. Moreover, one-loop electroweak corrections to the process $e^+e^- \rightarrow \nu\bar{\nu}A_0$ in the THDM have been computed in Ref. [20]. The CP-odd A_0 production at e^+e^- colliders in the MSSM with CP-violating phases have been computed in Ref. [21]. Additionally, the CP-odd Higgs boson production in association with a neutral gauge boson Z in high-energy e^+e^- collisions at one-loop level analyses has been reported in the frameworks of the THDM in Ref. [22] and supersymmetric models in Ref. [23].

In this paper, we present the first analytic expressions for one-loop contributions to the rare decay process $A_0 \rightarrow h_0h_0\gamma$ within the CP-conserving of the THDM. Analytic results are written in terms of scalar one-loop Passarino-Veltman functions (PV-functions) in the standard output of both packages `LoopTools` and `Collier`. Numerical checks for the validation of our calculations such as the ultraviolet and infrared finiteness, and the Ward identity of one-loop amplitude are also performed. In phenomenological results, the decay rates for $A_0 \rightarrow h_0h_0\gamma$ and the differential decay widths with respect to the invariant mass of Higgs-pair in final states are computed at several points of the allowed regions of the parameter space of the THDM. The paper is arranged as follows. In section 2, we briefly review the THDM. In section 3, the detailed evaluations for one-loop contributions to the decay channel $A_0 \rightarrow h_0h_0\gamma$ are presented. Phenomenological results for the calculations are shown in section 4. Important conclusions and outlook of this work are shown in section 5.

2. Two Higgs Doublet Models

We first review shortly the model under consideration in the calculation. For a complete review of this model and relevant phenomenological studies, we refer to Ref. [27]. In the structure of the THDM, fermion and gauge sectors are kept the same as those in the SM. With the above extension, the scalar potential, reflecting two gauge and Lorentz invariances, is written in a general form as follows

$$\begin{aligned} \mathcal{V}_{\text{THDM}}(\Phi_1, \Phi_2) = & m_{11}^2 \Phi_1^\dagger \Phi_1 + m_{22}^2 \Phi_2^\dagger \Phi_2 - \left[m_{12}^2 \Phi_1^\dagger \Phi_2 + \text{H.c.} \right] + \frac{\lambda_1}{2} (\Phi_1^\dagger \Phi_1)^2 + \frac{\lambda_2}{2} (\Phi_2^\dagger \Phi_2)^2 \\ & + \lambda_3 (\Phi_1^\dagger \Phi_1) (\Phi_2^\dagger \Phi_2) + \lambda_4 (\Phi_1^\dagger \Phi_2) (\Phi_2^\dagger \Phi_1) + \frac{1}{2} [\lambda_5 (\Phi_1^\dagger \Phi_2)^2 + \text{H.c.}]. \end{aligned} \quad (1)$$

Assuming the CP-conserving version of the THDM in this work, all bare parameters in the scalar potential are considered to be real. Additionally, the Z_2 -symmetry, e.g. $\Phi_1 \leftrightarrow \Phi_1$ and $\Phi_2 \leftrightarrow -\Phi_2$ is implied for the above scalar potential up to the allowed soft-breaking term given explicitly as $m_{12}^2 \Phi_1^\dagger \Phi_2 + \text{H.c.}$. The parameter m_{12}^2 plays a key role of the breaking scale for the Z_2 -symmetry.

For the EWSB, two scalar doublets are expanded around their VEVs as follows:

$$\Phi_k = \left[\begin{array}{c} \phi_k^+ \\ (v_k + \phi_k^0 + i\psi_k^0)/\sqrt{2} \end{array} \right] \quad \text{for } k = 1, 2. \quad (2)$$

The combined VEV is defined as $v = \sqrt{v_1^2 + v_2^2}$, which is fixed at $v \sim 246$ GeV in agreement with the SM limit. The physical particles in the THDM, after the EWSB, include two CP-even Higgs bosons, in which one of them is h_0 , being the SM-like Higgs boson found at the LHC, and another one is CP-even Higgs H . Furthermore, one also has a CP-odd Higgs (A_0) boson and a pair of charged Higgs bosons (H^\pm). The masses of all additional scalar bosons can be obtained subsequently by diagonalizing mass matrices in their favor bases. The rotations are shown in concrete as follows:

$$\begin{pmatrix} \phi_1^0 \\ \phi_2^0 \end{pmatrix} = \begin{pmatrix} c_\alpha & -s_\alpha \\ s_\alpha & c_\alpha \end{pmatrix} \begin{pmatrix} H \\ h_0 \end{pmatrix}, \quad (3)$$

$$\begin{pmatrix} \phi_1^\pm \\ \phi_2^\pm \end{pmatrix} = \begin{pmatrix} c_\beta & -s_\beta \\ s_\beta & c_\beta \end{pmatrix} \begin{pmatrix} G^\pm \\ H^\pm \end{pmatrix}, \quad (4)$$

$$\begin{pmatrix} \psi_1^0 \\ \psi_2^0 \end{pmatrix} = \begin{pmatrix} c_\beta & -s_\beta \\ s_\beta & c_\beta \end{pmatrix} \begin{pmatrix} G^0 \\ A_0 \end{pmatrix}. \quad (5)$$

The mixing angle β is given by $t_\beta \equiv \tan \beta = v_2/v_1$. In this circumstance, the neutral and singly charged Goldstone bosons, G^0 and G^\pm , give masses for gauge bosons Z and W^\pm , respectively. The physical masses of the remaining scalar bosons are then written in terms of the bare parameters as follows:

$$M_{H^\pm}^2 = M^2 - \frac{1}{2} \lambda_{45} v^2, \quad (6)$$

$$M_{A_0}^2 = M^2 - \lambda_5 v^2, \quad (7)$$

$$M_{h_0}^2 = M_{11}^2 s_{\beta-\alpha}^2 + M_{22}^2 c_{\beta-\alpha}^2 + M_{12}^2 s_{2(\beta-\alpha)}, \quad (8)$$

$$M_H^2 = M_{11}^2 c_{\beta-\alpha}^2 + M_{22}^2 s_{\beta-\alpha}^2 - M_{12}^2 s_{2(\beta-\alpha)}, \quad (9)$$

where $M^2 = m_{12}^2/(s_\beta c_\beta)$, and

$$M_{11}^2 = (\lambda_1 c_\beta^4 + \lambda_2 s_\beta^4) v^2 + \frac{v^2}{2} \lambda_{345} s_{2\beta}^2, \quad (10)$$

$$M_{22}^2 = M^2 + \frac{v^2}{4} [\lambda_{12} - 2\lambda_{345}] s_{2\beta}^2, \quad (11)$$

$$M_{12}^2 = M_{21}^2 = -\frac{v^2}{2} [\lambda_1 c_\beta^2 - \lambda_2 s_\beta^2 - \lambda_{345} c_{2\beta}] s_{2\beta}. \quad (12)$$

Here, the abbreviated notations $\lambda_{ij\dots} = \lambda_i + \lambda_j + \dots$ have been used for simplicity.

Lastly, we discuss the Yukawa sector in the THDM. It is well-known that the discrete Z_2 -symmetry is proposed in the THDM for avoiding Tree-level Flavor-Changing Neutral Currents (FCNCs). Based on the Z_2 -symmetry, the Yukawa interactions appearing in different THDMs are divided into four types, labeled as Type-I, -II, -X, and -Y, respectively, as shown in Table 1,

which precisely lists all the Z_2 charge assignments [28]. Accordingly, the Yukawa interactions are parameterized in the following general form:

$$\mathcal{L}_Y = - \sum_{f=u,d,\ell} \left(\frac{m_f}{\sqrt{2}v} \xi_h^f \bar{f} f h_0 + \frac{m_f}{\sqrt{2}v} \xi_H^f \bar{f} f H - i \frac{m_f}{v} \xi_A^f \bar{f} \gamma_5 f A_0 \right) - \left\{ \frac{\sqrt{2}V_{ud}}{v} \bar{u} (m_u \xi_A^u P_L + m_d \xi_A^d P_R) d H^+ + \frac{\sqrt{2}m_\ell \xi_A^\ell}{v} \bar{\nu}_L \ell_R H^+ + \text{H.c.} \right\}, \quad (13)$$

where projection operators are $P_{L(R)}$ for left (right)-handed of fermions. The elements V_{ud} of the Cabibbo-Kobayashi-Maskawa (CKM) matrix explaining the quark mixing also appear in the Yukawa Lagrangian.

Types	Φ_1	Φ_2	Q_L	L_L	u_R	d_R	e_R	ξ_A^u	ξ_A^d	ξ_A^ℓ	ξ_h^u	ξ_h^d	ξ_h^ℓ
I	+	-	+	+	-	-	-	$\cot \beta$	$-\cot \beta$	$\cot \beta$	$\frac{c_\alpha}{s_\beta}$	$\frac{c_\alpha}{s_\beta}$	$\frac{c_\alpha}{s_\beta}$
II	+	-	+	+	-	+	+	$-\cot \beta$	$-\tan \beta$	$-\tan \beta$	$\frac{c_\alpha}{s_\beta}$	$-\frac{c_\alpha}{s_\beta}$	$-\frac{c_\beta}{s_\alpha}$
X	+	-	+	+	-	-	+	$-\cot \beta$	$\cot \beta$	$-\tan \beta$	$\frac{c_\alpha}{s_\beta}$	$\frac{c_\alpha}{s_\beta}$	$-\frac{c_\beta}{s_\alpha}$
Y	+	-	+	+	-	+	-	$-\cot \beta$	$-\tan \beta$	$\cot \beta$	$\frac{c_\alpha}{s_\beta}$	$-\frac{c_\alpha}{s_\beta}$	$\frac{c_\beta}{s_\alpha}$

Table 1: The Z_2 charge assignments and $\xi_{A(h)}^f$ ($f = u, d, \ell$) factors corresponding to the four THDM types. While the Yukawa couplings of CP-even H to fermion pair (ξ_H^f) are obtained by replacing $c_\alpha \rightarrow s_\alpha$ and vice versa in ξ_h^f .

The parameter space $\mathcal{P}_{\text{THDM}}$ for THDM consists of the following free parameters:

$$\mathcal{P}_{\text{THDM}} = \{M_{h_0}^2 \sim 125 \text{ GeV}, M_H^2, M_{A_0}^2, M_{H^\pm}^2, m_{12}^2, t_\beta, s_{\beta-\alpha}\}. \quad (14)$$

To end this section, the current constraints on the parameter space of the THDM given in Eq. (14) are first summarized. For the subject, both theoretical and experimental constraints to the model are taken into consideration for finding the allowed parameter space of the THDM. In the theoretical perspectives, the requirements of the perturbative regime, the tree-level unitarity of gauge theory and the vacuum stability conditions of the scalar Higgs potential are taken into account [29, 30, 31, 32, 33]. From the experimental data, the EWPT for the THDM has implicated at the LEP as reported in Refs. [34, 35]. The bounds from indirect searches for the masses range of scalar particles in the THDM have studied in Ref. [36, 37, 38, 39]. Implicating one-loop induced for the SM-like Higgs decay channels like $h \rightarrow \gamma\gamma$ and $h \rightarrow Z\gamma$ in the context of THDM have examined in Refs. [44, 45]. Additionally, the implications of W -boson mass at the CDF-II in Refs. [40, 41, 42] and the updated constraints for muon $g-2$ anomaly in Ref. [43]. Lastly, the flavor experimental data as shown in Refs. [46, 47, 48] gives a further constraints on t_β , M_{H^\pm} . In detail, the results from Refs. [46, 47, 48] pointed out that the small values of t_β are favoured for explaining the flavor experimental data. For this reason, the small values for t_β are also considered for complementary discussion in this work. By considering all the above-constraints, we can take the physical parameters for the THDM in the regions like $126 \text{ GeV} \leq M_H \leq 1500 \text{ GeV}$, $60+ \text{ GeV} \leq M_A \leq 1500 \text{ GeV}$ and $80 \text{ GeV} \leq M_{H^\pm} \leq 1500 \text{ GeV}$. The Z_2 -breaking parameter can be taken as $m_{12}^2 = M_H^2 s_\beta c_\beta$. Our phenomenological results studied in the next sections will be examined in the above-mentioned parameter space.

3. Loop-induced decay of $A_0 \rightarrow h_0 h_0 \gamma$ in THDM

The detailed calculations for one-loop induced for the rare decay process $A_0 \rightarrow h_0 h_0 \gamma$ in the THDM are discussed in this section. The computations are handled with the help of the computer packages `FeynArts/FormCalc` [24]. One-loop analytic formulas are presented via scalar PV-functions following the standard output of the programs `LoopTools/Collider` [25, 26]. First, one-loop Feynman diagrams for the computed processes are generated automatically by using the package `FeynArts` within the 't Hooft-Feynman gauge (HF). In this computation, we employ on-shell renormalization scheme developed in Refs. [49, 50, 51] for both fermion sector and gauge sector. While the improved on-shell renormalization scheme is applied for the scalar Higgs sectors following in Ref. [52]. We list all one-loop induced Feynman diagrams for the channel $A_0 \rightarrow h_0 h_0 \gamma$. They are categorized into several groups showing in the next paragraphs. We first mention one-loop Feynman diagrams with A_0^* -pole as plotted in Fig. 1. These diagrams relating to off-shell decay process of $A_0^* \rightarrow h_0 \gamma$ in connection with the vertex $A_0^* A_0 h_0$. The second classification is included all Feynman diagrams with ϕ^* -poles for $\phi^* = h_0^*, H^*$ which are connected loop-induced processes $\phi^* \rightarrow h_0 \gamma$ with the vertex of $\phi^* h_0 h_0$, as plotted in Fig. 2. We next take into account all one-loop Feynman diagrams with Z^* -pole as shown in Fig. 3. In all the above-cases, we also have the mixing of Z - γ contributing to the considered process including for A^* -, ϕ^* - and Z^* -poles diagrams. Finally, we have one-loop four-point diagrams taking into consideration in this computed channel. For this group, we plot all one-loop four-legs topologies as in Fig. 4. We note that all particles like fermion f , vector bosons and scalar particles are considered to exchange in the loop diagrams. Within the HF gauge, the Goldstone and Ghost particles are also propagated in the loop. As indicated in latter, the fermion exchanging in the loop at several the above-groups gives zero contribution. For this reason, we skip showing fermion f in the loop accordingly in these corresponding groups.

In general, one-loop amplitude for the decay channel $A_0(p) \rightarrow h_0(k_1) h_0(k_2) \gamma_\mu(k_3)$ is given by following Lorentz structure as follows:

$$i\mathcal{M}_{A_0 \rightarrow h_0 h_0 \gamma} = \left[F_1 k_1^\mu + F_2 k_2^\mu \right] \varepsilon_\mu(k_3) \quad (15)$$

$$= F \left[\frac{k_1^\mu}{k_1 \cdot k_3} - \frac{k_2^\mu}{k_2 \cdot k_3} \right] \varepsilon_\mu(k_3), \quad (16)$$

where $\varepsilon_\mu(k_3)$ is the polarization vector of the external photon, three scalar factors F and $F_{1,2}$ are loop contributions. The amplitude in Eq. (15) follows the Ward identity relating to this on-shell final photon state, i.e., this amplitude will equal to zero after replacing $\varepsilon_\mu(k_3) \rightarrow k_{3,\mu}$. Subsequently, we derive the relation for F_1 , F_2 as follows:

$$F = (k_1 \cdot k_3) F_1 = -(k_2 \cdot k_3) F_2, \quad (17)$$

resulting in Eq. (16). More important, the decay amplitude under consideration can be calculated via one of the two form factors F_1 or F_2 . It means that we can collect form factor F as one of the coefficients of k_1^μ (or k_2^μ). One-loop form factor F is expressed as functions of following kinematic invariant masses:

$$p^2 = M_{A_0}^2, \quad k_1^2 = k_2^2 = M_{h_0}^2, \quad k_3^2 = 0, \quad k_{ij} = (k_i + k_j)^2, \quad \text{for } i, j = 1, 2, 3. \quad (18)$$

We have further relation as $k_{12} + k_{13} + k_{23} = 2M_{h_0}^2 + M_{A_0}^2$. We are going to present one-loop form factors in the next paragraphs. In general, one-loop form factors are decomposed into the

form of

$$\begin{aligned}
F(M_{A_0}^2, M_{h_0}^2; k_{12}, k_{13}, \dots) &= \frac{g_{h_0 A_0 A_0}}{k_{13} - M_{A_0}^2 + i\Gamma_{A_0} M_{A_0}} \cdot F_{A_0}^{(\text{Trig})} \\
&+ \sum_{\phi=\{h_0^*, H^*\}} \frac{g_{\phi h_0 h_0}}{k_{12} - M_\phi^2 + i\Gamma_\phi M_\phi} \cdot F_\phi^{(\text{Trig})} \\
&+ \sum_{ij=\{13, 23\}} \frac{g_{A_0 Z h_0}}{k_{ij}^2 - M_Z^2 + i\Gamma_Z M_Z} \cdot F_{Z,ij}^{(\text{Trig})} \\
&+ \sum_{N_S=\{S, SS, \dots\}} F_{(N_S, W)}^{(\text{Box})}.
\end{aligned} \tag{19}$$

Where general couplings are given

$$g_{h_0 A_0 A_0} = \frac{-ie}{2M_W s_\beta} \left[s_{\beta-\alpha} (2M_{A_0}^2 - M_{h_0}^2) + \frac{c_{\beta+\alpha}}{s_{2\beta}} \left(2M_{h_0}^2 - \frac{8M_W^2 s_W^2}{e^2 v^2} M^2 \right) \right], \tag{20}$$

$$g_{h_0 h_0 h_0} = \frac{-3ie}{2M_W s_W s_{2\beta}} \left[(2c_{\alpha+\beta} + s_{2\alpha} s_{\beta-\alpha}) M_{h_0}^2 - \frac{8M_W^2 s_W^2 c_{\beta+\alpha} c_{\beta-\alpha}}{e^2 v^2} M^2 \right], \tag{21}$$

$$g_{H h_0 h_0} = -\frac{[s_{2\alpha} (3M^2 - M_H^2 - 2M_{h_0}^2) - M^2 s_{2\beta}]}{v s_{2\beta}} c_{\alpha-\beta}, \tag{22}$$

$$g_{A_0 Z h_0} = \left(\frac{e}{2c_W s_W} \right) c_{\beta-\alpha}. \tag{23}$$

In the above equation, the first three form factors $F_{A_0}^{(\text{Trig})}$ and $F_\phi^{(\text{Trig})}$ ($F_{Z,ij}^{(\text{Trig})}$) correspond to the contributions from the A_0^* -pole and ϕ^* -pole (Z^* -pole) diagrams, respectively. While the remaining one-loop form factors calculated from one-loop four-point diagrams are decomposed into $F_{(S,W)}^{(\text{Box})}$, $F_{(SS,W)}^{(\text{Box})}$, $F_{(SSS,W)}^{(\text{Box})}$ terms by the numbers N_S of charged Higgs ($S \equiv H^\pm$) in the loop. In the box diagrams presenting in the computed processes, the maximum number of charged Higgs is $N_S = 3$ in internal lines.

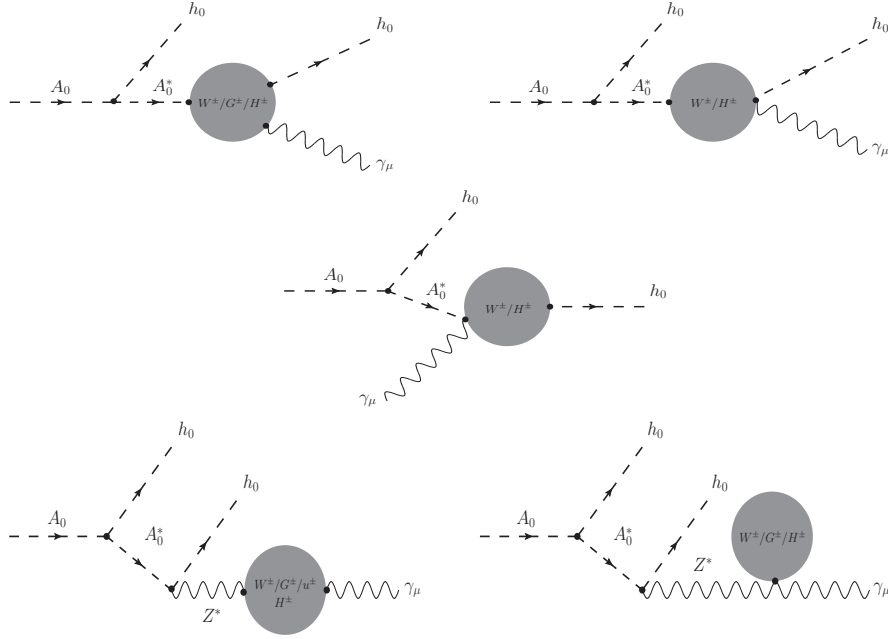


Figure 1: One-loop triangle diagrams including the mixing of Z - γ with A_0^* -pole. All particles like fermion f , vector bosons and scalar particles are considered to propagate in the loop diagrams. Within HF gauge, we have also Goldstone and Ghost particles exchanging in the loop.

We first show the factors collected from A_0^* -pole diagrams as shown in Feynman diagrams in Fig. 1. The resulting is presented in terms of scalar PV-functions as follows:

$$\begin{aligned}
\frac{F_{A_0}^{(\text{Trig})}}{k_1 \cdot k_3} &= -\frac{i e^3}{(4\pi)^2} \left(\frac{c_{\beta-\alpha}}{2M_W^2 s_W^2} \right) \left\{ M_W^2 \left[(B_1 - B_0)[M_{h_0}^2; H^\pm, W] - (5B_0 + B_1)[k_{13}; H^\pm, W] \right] \right. \\
&+ M_W^2 \left[4C_{00} + (M_{h_0}^2 + 3k_{13})C_{22} \right. \\
&+ (3M_{h_0}^2 + k_{13})C_{11} + 4(M_{h_0}^2 + k_{13})C_{12} \left. \right] [M_{h_0}^2, 0, k_{13}; H^\pm, W, W] \\
&+ \left[M_W^2 (3M_{h_0}^2 + 2M_{H^\pm}^2 - M_{A_0}^2 - 4M_W^2) + 2(M_{A_0}^2 - M_{H^\pm}^2)(M_{h_0}^2 - M_{H^\pm}^2) \right] \times \\
&\times C_0[M_{h_0}^2, 0, k_{13}; H^\pm, W, W] \\
&+ \left[M_{A_0}^2 (2M_{h_0}^2 - 2M_{H^\pm}^2 + M_W^2) - 2M_{h_0}^2 (M_{H^\pm}^2 - 5M_W^2) \right. \\
&+ 2M_{H^\pm}^2 (M_{H^\pm}^2 - M_W^2) - M_W^2 k_{13} \left. \right] C_1[M_{h_0}^2, 0, k_{13}; H^\pm, W, W] \\
&+ \left[M_W^2 (M_{A_0}^2 - 2M_{H^\pm}^2 + 4M_{h_0}^2 + 5k_{13}) + 2(M_{A_0}^2 - M_{H^\pm}^2)(M_{h_0}^2 - M_{H^\pm}^2) \right] \times \\
&\times C_2[M_{h_0}^2, 0, k_{13}; H^\pm, W, W] \\
&+ \left[2M_{A_0}^2 (M_{h_0}^2 - M_{H^\pm}^2) - 2M_W^2 k_{13} - 2M_{H^\pm}^2 (M_{h_0}^2 - M_{H^\pm}^2 + M_W^2) \right] \times \\
&\times C_2[0, k_{13}, M_{h_0}^2; H^\pm, H^\pm, W] \\
&+ 2M_W^2 \left[2C_{00} + (M_{h_0}^2 - k_{13})C_{12} + (M_{h_0}^2 + k_{13})C_{22} \right] [0, k_{13}, M_{h_0}^2; H^\pm, H^\pm, W] \left. \right\} \\
&- \frac{i e^3}{(4\pi)^2} \left(\frac{c_{\beta-\alpha}}{2M_Z^2 c_W s_W} \right) \cdot \Pi_{Z\gamma}[k_3^2 = 0, W^\pm, H^\pm], \tag{24}
\end{aligned}$$

where the two-point contribution relating to the Z - γ mixing is given in the following paragraph (as in Eq. (25)). Because of the appearance of the on-shell photon state, this two-point contribution at $k_3^2 = 0$ is only contributed from the charged Higgs and W bosons in the loop. In detail, the mixing is given by

$$\begin{aligned} \Pi_{Z\gamma}[k_3^2 = 0, W^\pm, H^\pm] &= \frac{2(M_Z^2 - 6M_W^2)}{M_W^2} \cot_W \left(A_0[W] - 2B_{00}[0; W, W] \right) \\ &+ 4M_Z^2 \cot_W B_0[0; W, W] \\ &+ 4 \cot_{2W} \left(-A_0[H^\pm] + 2B_{00}[0; H^\pm, H^\pm] \right). \end{aligned} \quad (25)$$

In the analytic expressions, the scalar one-loop coefficients $A_{ijk\dots}$, $B_{ijk\dots}$, $C_{ijk\dots}$ (and $D_{ijk\dots}$ appear in the later formulas) are so-called as the scalar PV-functions which are defined as in Ref. [55]. They are presented as standard output of both the packages `LoopTools` and `Collider`. In this work, the PV-functions are presented in the modified notations as:

$$\{A, B, C, D\}_{ijk\dots}[k_{ij}, \dots; M_A^2, M_B^2, M_C^2, \dots] = \{A, B, C, D\}_{ijk\dots}[k_{ij}, \dots; A, B, C, \dots]. \quad (26)$$

Where names of internal particles A, B, C, \dots stand for their invariant masses $M_A^2, M_B^2, M_C^2, \dots$, respectively.

One-loop form factors contributing from the diagrams with ϕ^* -poles for $\phi = h_0, H$ are next collected. One-loop Feynman diagrams for this group are plotted in Fig. 2.

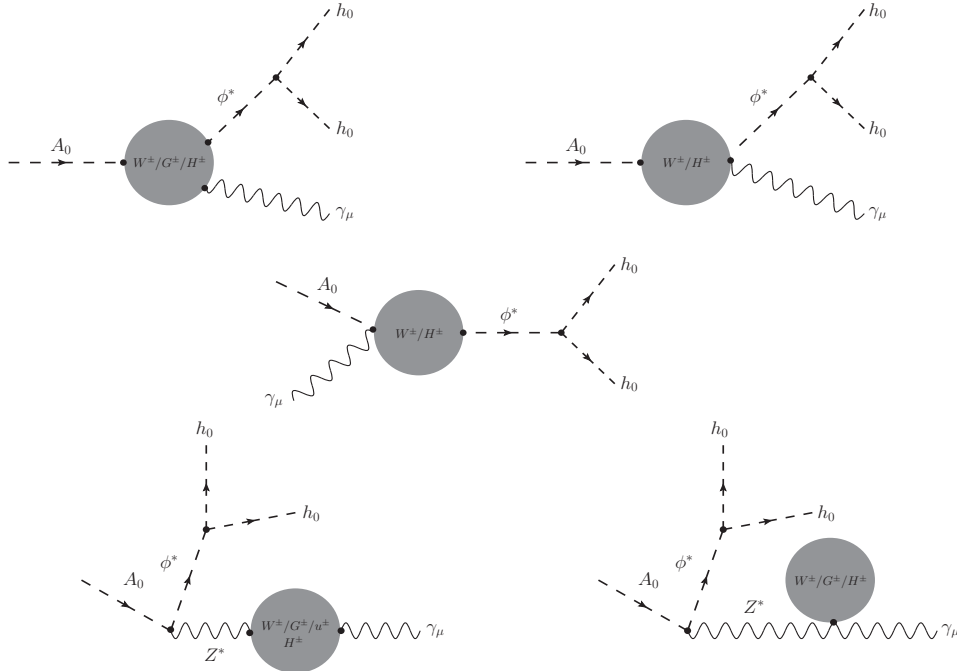


Figure 2: One-loop triangle diagrams with ϕ -poles for $\phi \equiv h_0, H$, including the mixing of Z - γ . All particles like fermion f , vector bosons and scalar particles are considered to propagate in the loop diagrams. Within HF gauge, we have also Goldstone and Ghost particles exchanging in the loop.

The corresponding factors are given in the form as follows:

$$\begin{aligned}
\frac{F_\phi^{(\text{Trig})}}{k_1 \cdot k_3} &= \frac{i e^2}{(4\pi)^2} \cdot \left(\frac{g_{\phi H^\pm W^\mp}}{M_W^2 s_W} \right) \left\{ M_W^2 (B_1 - B_0) [M_{A_0}^2; H^\pm, W] - M_W^2 (B_1 + 5B_0) [k_{12}; H^\pm, W] \right. \\
&+ M_W^2 \left[4C_{00} + (3M_{A_0}^2 + k_{12})C_{11} \right. \\
&+ 4(M_{A_0}^2 + k_{12})C_{12} + (M_{A_0}^2 + 3k_{12})C_{22} \left. \right] [M_{A_0}^2, 0, k_{12}; H^\pm, W, W] \\
&+ \left[M_W^2 (3M_{A_0}^2 - M_\phi^2 + 2M_{H^\pm}^2 - 4M_W^2) + 2(M_{A_0}^2 - M_{H^\pm}^2)(M_\phi^2 - M_{H^\pm}^2) \right] \times \\
&\times C_0 [M_{A_0}^2, 0, k_{12}; H^\pm, W, W] \\
&+ \left[2M_{A_0}^2 (M_\phi^2 - M_{H^\pm}^2 + 5M_W^2) - M_\phi^2 (2M_{H^\pm}^2 - M_W^2) \right. \\
&\quad \left. - 2M_{H^\pm}^2 (M_W^2 - M_{H^\pm}^2) - M_W^2 k_{12} \right] C_1 [M_{A_0}^2, 0, k_{12}; H^\pm, W, W] \\
&+ \left[2(M_{A_0}^2 - M_{H^\pm}^2)(M_\phi^2 - M_{H^\pm}^2) + M_W^2 (4M_{A_0}^2 - 2M_{H^\pm}^2 + M_\phi^2 + 5k_{12}) \right] \times \\
&\times C_2 [M_{A_0}^2, 0, k_{12}; H^\pm, W, W] \\
&+ 2M_W^2 \left[(M_{A_0}^2 - k_{12})C_{12} + (k_{12} + M_{A_0}^2)C_{22} + 2C_{00} \right] [0, k_{12}, M_{A_0}^2; H^\pm, H^\pm, W] \\
&+ \left. \left[2(M_{A_0}^2 - M_{H^\pm}^2)(M_\phi^2 - M_{H^\pm}^2) - 2M_W^2 (M_{H^\pm}^2 + k_{12}) \right] C_2 [0, k_{12}, M_{A_0}^2; H^\pm, H^\pm, W] \right\} \\
&+ \frac{i e^2}{(4\pi)^2} \left(\frac{g_{A_0 Z \phi}}{M_Z^2 s_{2W}} \right) \cdot \Pi_{Z\gamma} [k_3^2 = 0, W^\pm, H^\pm]. \tag{27}
\end{aligned}$$

Where the general couplings are shown as $g_{A_0 Z \phi} = \frac{e c_{\beta-\alpha}}{2c_W s_W} \left(-\frac{e s_{\beta-\alpha}}{2c_W s_W} \right)$ for $\phi = h_0$ (H), respectively. Other general couplings are presented as $g_{\phi H^\pm W^\mp} = \frac{-ie c_{\beta-\alpha}}{2s_W} \left(\frac{ie s_{\beta-\alpha}}{2s_W} \right)$ for $\phi = h_0$ (H), correspondingly. In further, the mixing Z - γ is also given by Eq. (25).

We next consider one-loop triangle diagrams with Z -pole including the mixing of Z - γ attributing to one-loop form factors. All internal particles such as fermion, vector bosons, scalar particles are considered exchanging in the loop. These diagrams are plotted in Fig. 3.

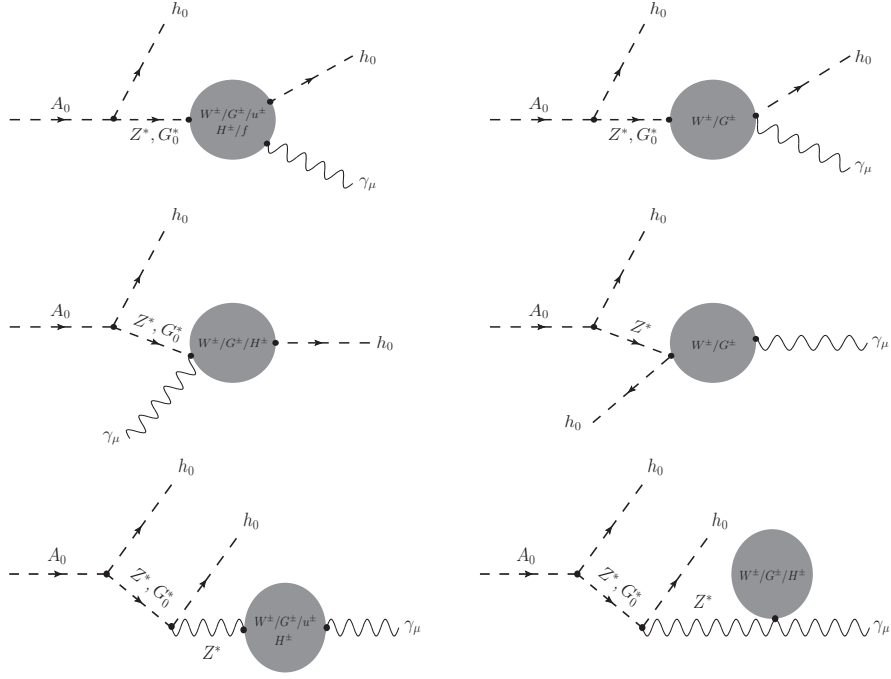


Figure 3: One-loop triangle diagrams with Z -pole including the mixing of Z - γ .

There are two form factors relating to the contributions of Z -pole giving in the above equation like $F_{Z,13}^{(\text{Trig})}$ and $F_{Z,23}^{(\text{Trig})}$. Different from the previous form factors, both factors for Z -pole have non-zero contributions from fermion f exchanging in the loop. We show the analytic results for one-loop form factors $F_{Z,ij}^{(\text{Trig})}$ as follows:

$$F_{Z,ij}^{(\text{Trig})} = \sum_{P=\{f,W,H^\pm\}} F_{Z,ij}^{(\text{Trig},P)} + F_{Z,ij}^{(Z-\gamma)} \quad (28)$$

for $ij = \{13, 23\}$. Where each factor is given accordingly:

$$\begin{aligned} \frac{F_{Z,13}^{(\text{Trig},f)}}{k_1 \cdot k_3} &= - \sum_f \frac{e Q_f N_C^f m_f^2}{2\pi^2} g_{h_0 f \bar{f}} \times g_{Z f \bar{f}} \times \\ &\times \left\{ B_0[k_{13}; f, f] + \left[2(3M_{h_0}^2 - 2k_{12} - k_{13})C_{11} - 2(3M_{h_0}^2 - 2k_{23} - k_{13})C_{12} \right. \right. \\ &\left. \left. + (M_{h_0}^2 - 2k_{12} + 2k_{23} - k_{13})C_1 - (M_{h_0}^2 - k_{23})C_0 - 4C_{00} \right] [M_{h_0}^2, k_{13}, 0; f, f, f] \right\}. \end{aligned} \quad (29)$$

Here N_C^f stands for number for color of the corresponding fermion f . It will be 1 for leptons and 3 for quarks. The general coupling $g_{h_0 f \bar{f}}$ is given in Table 1 in the section 2. While $g_{Z f \bar{f}}$ are

couplings of Z with fermion-pair which are taken in the SM. Other factors are presented as:

$$\begin{aligned}
\frac{F_{Z,13}^{(\text{Trig},W)}}{k_1 \cdot k_3} &= \frac{e^3}{(4\pi)^2} \frac{c_W s_{\beta-\alpha}}{2M_W^2 s_W^2} \left\{ 2M_W^2 (M_W^2 - M_Z^2) B_0[0; W, W] \right. \\
&+ \left\{ M_W^2 (M_{h_0}^2 - M_{A_0}^2) B_1 \right. \\
&+ \left[M_W^2 (M_{A_0}^2 + 12M_W^2) + M_{h_0}^2 (M_W^2 - M_Z^2) \right] B_0 \left. \right\} [M_{h_0}^2; W, W] \\
&+ M_W^2 \left[3(M_{h_0}^2 - M_{A_0}^2) (B_1 - B_0) - 2(M_W^2 + 2M_Z^2) B_0 \right] [k_{13}; W, W] \\
&- 4 \left[2M_W^2 (M_{A_0}^2 + 6M_W^2) - M_Z^2 (M_{h_0}^2 + 2M_W^2) \right] C_{00} [M_{h_0}^2, k_{13}, 0; W, W, W] \\
&+ 2M_W^2 \left[3M_W^2 (M_{A_0}^2 - M_{h_0}^2 - M_Z^2) + 2M_{h_0}^2 (M_{A_0}^2 - M_{h_0}^2 - 4M_W^2) \right. \\
&+ k_{12} (M_Z^2 - 3M_W^2) \\
&+ k_{13} (M_{h_0}^2 - M_{A_0}^2 + M_Z^2) + k_{23} (13M_W^2 - 3M_Z^2) \left. \right] C_0 [M_{h_0}^2, k_{13}, 0; W, W, W] \\
&+ \left\{ M_W^2 \left[M_{h_0}^2 (11M_{h_0}^2 - 5M_{A_0}^2 + 60M_W^2) \right. \right. \\
&+ k_{13} (M_{h_0}^2 - 3M_{A_0}^2 - 20M_W^2) - 4k_{12} (M_{h_0}^2 + 10M_W^2) \left. \right] \\
&+ 2(M_{h_0}^2 + 2M_W^2) (M_W^2 - M_Z^2) (3M_{h_0}^2 - 2k_{12} - k_{13}) \left. \right\} C_{11} [M_{h_0}^2, k_{13}, 0; W, W, W] \\
&- 2 \left[M_{h_0}^2 M_W^2 (2M_{A_0}^2 + M_{h_0}^2 + 30M_W^2) \right. \\
&- M_W^2 k_{13} (2M_{A_0}^2 - M_{h_0}^2 + 10M_W^2) - 2M_W^2 k_{23} (M_{h_0}^2 + 10M_W^2) \\
&+ (M_{h_0}^2 + 2M_W^2) (M_W^2 - M_Z^2) (3M_{h_0}^2 - k_{13} - 2k_{23}) \left. \right] C_{12} [M_{h_0}^2, k_{13}, 0; W, W, W] \\
&+ \left\{ M_{h_0}^2 M_W^2 (4M_{A_0}^2 - 4M_{h_0}^2 - 4M_W^2 - 9M_Z^2) + M_W^2 k_{13} (M_{h_0}^2 + M_Z^2 - M_{A_0}^2) \right. \\
&+ k_{12} \left[(2M_{h_0}^2 + 5M_W^2) (M_Z^2 - M_W^2) - M_W^2 (19M_W^2 + 2M_{h_0}^2) \right] \\
&+ k_{23} \left[(2M_{h_0}^2 + 3M_W^2) (M_W^2 - M_Z^2) + M_W^2 (2M_{h_0}^2 + 21M_W^2) \right] \left. \right\} \times \\
&\times C_1 [M_{h_0}^2, k_{13}, 0; W, W, W] \\
&+ \left. \left[2M_W^2 (M_{h_0}^2 - k_{13}) (2M_{A_0}^2 - 2M_{h_0}^2 - M_W^2 - M_Z^2) \right] C_2 [M_{h_0}^2, k_{13}, 0; W, W, W] \right\},
\end{aligned} \tag{30}$$

$$\begin{aligned}
\frac{F_{Z,13}^{(\text{Trig},H^\pm)}}{k_1 \cdot k_3} &= -\frac{ie^2}{(4\pi)^2} \frac{\cot_{2W}}{2M_W^4} \cdot g_{h_0 H^\pm H^\mp} \times \\
&\times \left\{ -4M_W^4 B_0 [M_{h_0}^2; H^\pm, H^\pm] + 8M_W^4 \left[2C_{00} - (3M_{h_0}^2 - 2k_{12} - k_{13}) C_{11} \right. \right. \\
&+ \left. \left. (3M_{h_0}^2 - k_{13} - 2k_{23}) C_{12} + (k_{12} - k_{23}) C_1 \right] [M_{h_0}^2, k_{13}, 0; H^\pm, H^\pm, H^\pm] \right\},
\end{aligned} \tag{31}$$

$$\frac{F_{Z,13}^{(Z-\gamma)}}{k_1 \cdot k_3} = -\frac{e^3}{(4\pi)^2} \frac{M_W s_{\beta-\alpha}}{s_W c_W^2} \left(\frac{M_{h_0}^2 - M_{A_0}^2 + M_Z^2}{4M_Z^4} \right) \cdot \Pi_{Z\gamma} [k_3^2 = 0, W^\pm, H^\pm]. \tag{32}$$

Other factors collected from Z -pole diagrams are given by

$$\frac{F_{Z,23}^{(\text{Trig},f)}}{k_1 \cdot k_3} = - \sum_f \frac{eQ_f N_C^f \times m_f^2}{2\pi^2} g_{h_0 f \bar{f}} \times g_{Z f \bar{f}} \times \quad (33)$$

$$\times \left\{ 2B_0[k_{23}; f, f] + \left[(M_{h_0}^2 - k_{23})(C_0 + 2C_1) - 8C_{00} \right] [M_{h_0}^2, k_{23}, 0; f, f, f] \right\},$$

$$\frac{F_{Z,23}^{(\text{Trig},W)}}{k_1 \cdot k_3} = \frac{e^3}{(4\pi)^2} \frac{c_W s_{\beta-\alpha}}{M_W^3 s_W^2} \left\{ 2M_W^2 (M_W^2 - M_Z^2) B_0[0; W, W] \quad (34)$$

$$+ \left[M_{h_0}^2 (2M_W^2 - M_Z^2) + 12M_W^4 \right] B_0[M_{h_0}^2; W, W]$$

$$- 2M_W^2 (M_W^2 + 2M_Z^2) B_0[k_{23}; W, W]$$

$$- 4 \left[(M_{h_0}^2 + 2M_W^2)(2M_W^2 - M_Z^2) + 8M_W^4 \right] C_{00}[M_{h_0}^2, k_{23}, 0; W, W, W]$$

$$+ 2M_W^2 \left[M_{h_0}^2 (7M_W^2 - 3M_Z^2) + k_{23}(2M_Z^2 - 5M_W^2) - 3M_Z^2 M_W^2 \right] \times$$

$$\times C_0[M_{h_0}^2, k_{23}, 0; W, W, W]$$

$$- 2M_W^2 \left[M_{h_0}^2 (2M_W^2 + 3M_Z^2) - M_Z^2 k_{23} \right] C_1[M_{h_0}^2, k_{23}, 0; W, W, W]$$

$$- \left[2M_W^2 (M_{h_0}^2 - k_{23})(M_W^2 + M_Z^2) \right] C_2[M_{h_0}^2, k_{23}, 0; W, W, W] \Big\},$$

$$\frac{F_{Z,23}^{(\text{Trig},H^\pm)}}{k_1 \cdot k_3} = - \frac{ie^2}{(4\pi)^2} \left(\frac{\cot_2 W}{M_W^4} \right) \cdot g_{h_0 H^\pm H^\mp} \times \quad (35)$$

$$\times \left\{ - 4M_W^4 B_0[M_{h_0}^2; H^\pm, H^\pm] + 16M_W^4 C_{00}[M_{h_0}^2, k_{23}, 0; H^\pm, H^\pm, H^\pm] \right\},$$

$$\frac{F_{Z,23}^{(Z-\gamma)}}{k_1 \cdot k_3} = - \frac{e^3 M_W s_{\beta-\alpha}}{(4\pi)^2 s_W c_W^2} \left(\frac{1}{M_Z^2} \right) \cdot \Pi_{Z\gamma}[k_3^2 = 0, W^\pm, H^\pm]. \quad (36)$$

Where the general coupling given in the above equations

$$g_{h_0 H^\pm H^\mp} = - \frac{c_{\alpha+\beta}(4M^2 - 3M_h^2 - 2M_{H^\pm}^2) + (2M_{H^\pm}^2 - M_h^2)c_{(\alpha-3\beta)}}{2v s_2 \beta} \quad (37)$$

is taken as in Ref. [53]. Here the mixing of Z - γ is also used the equation (25).

We turn our attention to the contributions from one-loop four-point Feynman diagrams. All the diagrams plotted within the HF gauge are shown in the below paragraphs. We confirm that the contributions from fermion f in the loop of all one-loop box diagrams are vanished in this case.

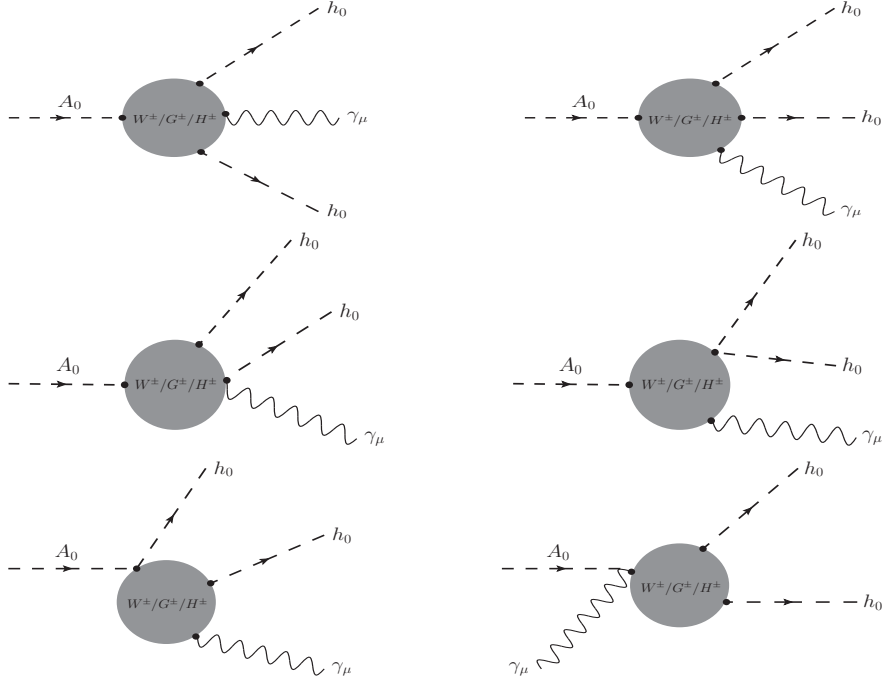


Figure 4: One-loop four-point Feynman diagrams contributing to the considered processes. We only have charged Higgses and W bosons together with Goldstone bosons in HF gauge are considered to exchange in the loop.

One-loop form factors $F_{(S\dots,W)}^{(\text{Box})}$ are collected from one-loop four-point diagrams which are divided into sub-factors following number of charged Higgses in the loop. We first present the factors deriving from the diagrams with one charged Higgs in the loop. The factors are taken in the form of

$$\frac{F_{(S,W)}^{(\text{Box})}}{k_1 \cdot k_3} = \frac{e^2}{8\pi^2} \left(\frac{g_{h_0 h_0 H^\pm G^\mp}}{2M_W s_W} \right) \cdot G_0 + \frac{e^4}{32\pi^2} \left(\frac{s_{2(\beta-\alpha)}}{M_W^3 s_W s_{2W}^2} \right) \cdot \sum_{i=1}^5 G_i. \quad (38)$$

The general coupling $g_{h_0 h_0 H^\pm G^\mp}$ is taken into account in the above equation (this coupling is collected as in Ref. [53]) as follows

$$g_{h_0 h_0 H^\pm G^\mp} = \frac{e^2 c_{\beta-\alpha}}{4M_W^2 s_W^2 s_{2\beta}} \left\{ 2c_{\alpha+\beta} (M_{h_0}^2 - M^2) + s_{\beta-\alpha} \left[s_{2\alpha} (M_{h_0}^2 - M_{H_0}^2) - 2s_{2\beta} (M_{H^\pm}^2 - M^2) \right] \right\}. \quad (39)$$

All factors G_i for $i = 0, 1, \dots, 5$ are listed in terms of PV-functions as follows

$$\begin{aligned} \frac{G_0}{M_W^2} &= \frac{[2M_{H^\pm}^2 - 2M_{A_0}^2 + M_W^2]}{M_W^2} C_0[M_{A_0}^2, 0, k_{12}; H^\pm, W, W] \\ &+ \frac{[2M_{H^\pm}^2 - 2M_{A_0}^2 - M_W^2]}{M_W^2} (C_1 + C_2)[M_{A_0}^2, 0, k_{12}; H^\pm, W, W]. \end{aligned} \quad (40)$$

Another factor is given by

$$\begin{aligned}
\frac{G_1}{M_W^2} = & \left[2M_W^2 C_0 - (M_{h_0}^2 - M_{H^\pm}^2 + 2M_W^2)(C_1 + 2C_2) \right] [M_{h_0}^2, M_{h_0}^2, k_{12}; H^\pm, W, W] \\
& - \left[2(M_{A_0}^2 - M_{H^\pm}^2 - M_W^2)C_0 + (M_{A_0}^2 - M_{H^\pm}^2 + 2M_W^2)C_1 \right] [M_{A_0}^2, M_{h_0}^2, k_{23}; H^\pm, W, W] \\
& - \left[(M_{A_0}^2 - M_{H^\pm}^2 - 2M_W^2)C_0 \right. \\
& \left. + (M_{A_0}^2 - M_{H^\pm}^2 + 2M_W^2)(C_1 + C_2) \right] [M_{A_0}^2, M_{h_0}^2, k_{13}; H^\pm, W, W] \\
& + (M_{A_0}^2 + M_{h_0}^2 - 2M_{H^\pm}^2)(C_0 - C_1 - C_2) [M_{h_0}^2, k_{23}, M_{A_0}^2; H^\pm, W, W] \\
& + \left[(M_{h_0}^2 - M_{H^\pm}^2)C_0 - (M_{A_0}^2 + M_{h_0}^2 - 2M_{H^\pm}^2)C_2 \right] [M_{h_0}^2, k_{13}, M_{A_0}^2; H^\pm, W, W] \\
& - 2(M_{A_0}^2 - M_{H^\pm}^2 - M_W^2)C_0 [k_{23}, 0, M_{h_0}^2; H^\pm, W, W] \\
& + \left[(2M_{A_0}^2 + 4M_{h_0}^2 - 6M_{H^\pm}^2 + 5M_W^2)C_0 \right. \\
& \left. + (2M_{A_0}^2 - 2M_{H^\pm}^2 + M_W^2)(C_1 + C_2) \right] [M_{h_0}^2, 0, k_{13}; W, W, W] \\
& + 2(M_{h_0}^2 + M_{A_0}^2 - 2M_{H^\pm}^2 + 6M_W^2)C_0 [M_{h_0}^2, 0, k_{23}; W, W, W] \\
& + \frac{(M_{A_0}^2 - M_{H^\pm}^2)}{M_W^2} \left[(-2M_{h_0}^2 + 2M_{H^\pm}^2 + M_W^2)C_0 \right. \\
& \left. - (2M_{h_0}^2 - 2M_{H^\pm}^2 + M_W^2)(C_1 + C_2) \right] [M_{h_0}^2, 0, k_{13}; H^\pm, W, W], \tag{41}
\end{aligned}$$

and

$$\begin{aligned}
\frac{G_2}{M_W^2} = & \left\{ (-2M_{A_0}^2 + 2M_{H^\pm}^2 - 8M_W^2)D_{00} + \left[-2M_{h_0}^2(-2M_{h_0}^2 + M_W^2 + k_{12}) \right. \right. \\
& \left. \left. + k_{12}(M_{H^\pm}^2 - 2M_W^2) + M_{A_0}^2(k_{12} - 4M_{h_0}^2) - 2M_W^2 k_{13} \right] D_{11} \right. \\
& + \left[(M_{A_0}^2 - 8M_{h_0}^2 + M_{H^\pm}^2 - 2M_W^2 + k_{12} - 2k_{13})M_{A_0}^2 - 6M_W^2 k_{13} \right. \\
& \left. + k_{12}(M_{H^\pm}^2 - 2M_W^2) - 2M_{h_0}^2(-3M_{h_0}^2 + M_W^2 + k_{12} - k_{13}) \right] D_{12} \\
& + \left[(M_{A_0}^2 + M_{H^\pm}^2 - 4M_W^2 - k_{12} - 2k_{13})M_{A_0}^2 + k_{12}(M_{H^\pm}^2 - 2M_W^2) \right. \\
& \left. - 2M_W^2 k_{13} + 2M_{h_0}^2(-M_{h_0}^2 + M_W^2 + k_{13}) \right] D_{33} \\
& + \left[-(4M_{h_0}^2 - 2M_{A_0}^2 - 2M_{H^\pm}^2 + 6M_W^2 + k_{12} + 4k_{13})M_{A_0}^2 \right. \\
& \left. + k_{12}(M_{H^\pm}^2 - 2M_W^2) - 6M_W^2 k_{13} + 2M_{h_0}^2(M_W^2 + 2k_{13}) \right] D_{23} \\
& + \left[(-4M_{h_0}^2 + M_{A_0}^2 + M_{H^\pm}^2 - 2M_W^2 - 2k_{13})M_{A_0}^2 \right. \\
& \left. + 2M_{h_0}^2(M_{h_0}^2 + k_{13}) - 4M_W^2 k_{13} \right] D_{22} \\
& + \left[(-4M_{h_0}^2 + M_{A_0}^2 + M_{H^\pm}^2 - 4M_W^2 - 2k_{13})M_{A_0}^2 + 2M_{h_0}^2(M_{h_0}^2 + k_{13} - k_{12}) \right. \\
& \left. + 2M_{H^\pm}^2 k_{12} - 4M_W^2(k_{12} + k_{13}) \right] D_{13} \left. \right\} [M_{h_0}^2, 0, M_{h_0}^2, M_{A_0}^2; k_{13}, k_{23}; H^\pm, W, W, W]
\end{aligned}$$

$$\begin{aligned}
& + \frac{1}{M_W^2} \left\{ \left[M_{h_0}^2 (-2M_{h_0}^2 + 2M_{H^\pm}^2 + M_W^2) + M_W^2 (4M_{H^\pm}^2 - M_{A_0}^2 + M_W^2 + k_{13}) \right] M_{A_0}^2 \right. \\
& + 2M_{h_0}^4 (M_{H^\pm}^2 + M_W^2) + M_{H^\pm}^2 M_W^2 (-5M_{H^\pm}^2 + 5M_W^2 + k_{13}) \\
& \left. - M_{h_0}^2 \left[(2M_{H^\pm}^2 + M_W^2) M_{H^\pm}^2 + 2M_W^2 k_{13} \right] \right\} D_0[M_{h_0}^2, 0, M_{h_0}^2, M_{A_0}^2; k_{13}, k_{23}; H^\pm, W, W, W] \\
& + \frac{1}{M_W^2} \left\{ -M_{A_0}^2 \left[M_{h_0}^2 (2M_{h_0}^2 - 2M_{H^\pm}^2 + M_W^2) + M_W^2 (-M_{A_0}^2 + M_W^2 + k_{12} + k_{13}) \right] \right. \\
& + 2M_{h_0}^4 (M_{H^\pm}^2 + 3M_W^2) + M_W^2 \left[3M_{H^\pm}^2 (-M_{H^\pm}^2 + M_W^2 + k_{12} + k_{13}) + 2M_W^2 (k_{12} + k_{13}) \right] \\
& \left. - M_{h_0}^2 \left[(2M_{H^\pm}^2 + 3M_W^2) M_{H^\pm}^2 + 2M_W^2 (3M_W^2 + k_{12} + k_{13}) \right] \right\} \times \\
& \times D_1[M_{h_0}^2, 0, M_{h_0}^2, M_{A_0}^2; k_{13}, k_{23}; H^\pm, W, W, W] \\
& + \frac{1}{M_W^2} \left\{ -M_{A_0}^2 \left[(2M_{h_0}^2 + M_W^2 - 2M_{H^\pm}^2) M_{h_0}^2 + M_W^2 (M_{H^\pm}^2 + 3M_W^2 + 4k_{12} + 3k_{13}) \right] \right. \\
& + 2M_{h_0}^4 (M_{H^\pm}^2 + 2M_W^2) - M_{h_0}^2 \left[M_{H^\pm}^2 (2M_{H^\pm}^2 + 3M_W^2) + 4M_W^4 \right] \\
& \left. + M_W^2 \left[4M_{A_0}^4 + M_{H^\pm}^2 (-3M_{H^\pm}^2 + 3M_W^2 + 4k_{12} + 3k_{13}) + 4M_W^2 k_{12} \right] \right\} \times \\
& \times D_2[M_{h_0}^2, 0, M_{h_0}^2, M_{A_0}^2; k_{13}, k_{23}; H^\pm, W, W, W] \\
& + \frac{1}{M_W^2} \left\{ -M_{A_0}^2 \left[M_W^2 (M_{H^\pm}^2 + 5M_W^2 + 3k_{12} + 3k_{13}) - 4M_W^2 M_{A_0}^2 \right. \right. \\
& \left. - M_{h_0}^2 (2M_{H^\pm}^2 - 2M_{h_0}^2 + 3M_W^2) \right] - M_{h_0}^2 \left[M_{H^\pm}^2 (2M_{H^\pm}^2 - 2M_{h_0}^2 + 3M_W^2) + 2M_W^4 \right] \\
& \left. + M_W^2 \left[3M_{H^\pm}^2 (M_W^2 - M_{H^\pm}^2 + k_{12} + k_{13}) + 2M_W^2 (k_{12} + k_{13}) \right] \right\} \times \\
& \times D_3[M_{h_0}^2, 0, M_{h_0}^2, M_{A_0}^2; k_{13}, k_{23}; H^\pm, W, W, W]. \tag{42}
\end{aligned}$$

Next, coefficient factors G_3 , G_4 and G_5 are expressed as follows:

$$\begin{aligned}
\frac{G_3}{M_W^2} = & \left\{ (-2M_{h_0}^2 + 2M_{H^\pm}^2 - 8M_W^2)D_{00} \right. \\
& - \left[2k_{12}(M_{h_0}^2 + 2M_W^2) + M_{A_0}^2(M_{h_0}^2 - M_{H^\pm}^2 + 2M_W^2 - 2k_{12}) \right] D_{22} \\
& + \left[(3M_{h_0}^2 + M_{H^\pm}^2 - 2M_W^2 - 2k_{12} - k_{13})M_{h_0}^2 \right. \\
& - 2M_W^2 k_{12} + M_{A_0}^2(2k_{12} - 4M_{h_0}^2) + (M_{H^\pm}^2 - 2M_W^2)k_{13} \left. \right] D_{11} \\
& + \left[(3M_{h_0}^2 + M_{H^\pm}^2 - 2M_W^2 - 4k_{12} - k_{13})M_{h_0}^2 + (M_{H^\pm}^2 - 2M_W^2)k_{13} \right. \\
& - 6M_W^2 k_{12} + M_{A_0}^2(-5M_{h_0}^2 + M_{H^\pm}^2 - 2M_W^2 + 4k_{12}) \left. \right] D_{12} \\
& - \left[2M_{A_0}^2(-M_{A_0}^2 + M_{h_0}^2 - M_{H^\pm}^2 + 3M_W^2 - k_{12} + k_{13}) + (2M_W^2 - M_{H^\pm}^2)k_{13} \right. \\
& + 6M_W^2 k_{12} + M_{h_0}^2(M_{H^\pm}^2 + M_{h_0}^2 - 2M_W^2 + 2k_{12} - k_{13}) \left. \right] D_{23} \\
& + \left[(-5M_{h_0}^2 + 2M_{A_0}^2 + M_{H^\pm}^2 - 4M_W^2 + 2k_{12} - 2k_{13})M_{A_0}^2 \right. \\
& + 2M_{h_0}^2(M_{h_0}^2 - k_{12}) + 2k_{13}(M_{H^\pm}^2 - 2M_W^2) - 4M_W^2 k_{12} \left. \right] D_{13} \\
& - \left[(-2M_{A_0}^2 + M_{h_0}^2 - M_{H^\pm}^2 + 4M_W^2 + 2k_{13})M_{A_0}^2 + 2M_W^2 k_{12} + (2M_W^2 - M_{H^\pm}^2)k_{13} \right. \\
& + M_{h_0}^2(M_{H^\pm}^2 + M_{h_0}^2 - 2M_W^2 - k_{13}) \left. \right] D_{33} \left. \right\} [M_{h_0}^2, M_{h_0}^2, 0, M_{A_0}^2; k_{12}, k_{23}; H^\pm, W, W, W] \\
& + \frac{1}{M_W^2} \left\{ \left[M_{h_0}^2(2M_{H^\pm}^2 + M_W^2) - 2M_{H^\pm}^4 + M_W^2(k_{12} - M_W^2) \right] M_{h_0}^2 \right. \\
& - M_{H^\pm}^2 M_W^2(5M_{H^\pm}^2 - 5M_W^2 - k_{12}) + M_{A_0}^2 \left[M_{h_0}^2(-2M_{h_0}^2 + 2M_{H^\pm}^2 + M_W^2) \right. \\
& + M_W^2(3M_{H^\pm}^2 + 2M_W^2 - 2k_{12}) \left. \right] \left. \right\} D_0[M_{h_0}^2, M_{h_0}^2, 0, M_{A_0}^2; k_{12}, k_{23}; H^\pm, W, W, W] \\
& + \frac{1}{M_W^2} \left\{ 2M_W^2 M_{A_0}^4 - 2M_{A_0}^2 \left[M_W^2(3M_W^2 + k_{12} + k_{13}) - M_{h_0}^2(-M_{h_0}^2 + M_{H^\pm}^2 + 2M_W^2) \right] \right. \\
& + 2M_{h_0}^4 M_{H^\pm}^2 + M_W^2 \left[-3M_{H^\pm}^4 + 3(M_W^2 + k_{12} + k_{13})M_{H^\pm}^2 + 2M_W^2(k_{12} + k_{13}) \right] \\
& - M_{h_0}^2 \left[2M_{H^\pm}^4 + 3M_W^2 M_{H^\pm}^2 + M_W^2(M_W^2 + k_{12} + k_{13}) \right] \left. \right\} \times \\
& \times D_3[M_{h_0}^2, M_{h_0}^2, 0, M_{A_0}^2; k_{12}, k_{23}; H^\pm, W, W, W] \\
& + \frac{1}{M_W^2} \left\{ -M_{h_0}^2 \left[2M_{H^\pm}^4 + 4M_W^2 M_{H^\pm}^2 + M_W^2(3M_W^2 + 3k_{12} + 4k_{13}) \right] \right. \\
& + M_{h_0}^4(2M_{H^\pm}^2 + 3M_W^2) - 2M_{A_0}^2 \left[M_{h_0}^4 - (M_{H^\pm}^2 + 2M_W^2)M_{h_0}^2 + 2M_W^4 \right] \\
& + M_W^2 \left[-3M_{H^\pm}^4 + (3M_W^2 + 3k_{12} + 4k_{13})M_{H^\pm}^2 + 4M_W^2 k_{13} \right] \left. \right\} \times \\
& \times D_2[M_{h_0}^2, M_{h_0}^2, 0, M_{A_0}^2; k_{12}, k_{23}; H^\pm, W, W, W]
\end{aligned}$$

$$\begin{aligned}
& + \frac{1}{M_W^2} \left\{ 2M_{h_0}^4 (M_{H^\pm}^2 + 4M_W^2) \right. \\
& - \left[(2M_{H^\pm}^2 + 5M_W^2)M_{H^\pm}^2 + M_W^2(5M_W^2 + 3k_{12} + 3k_{13}) \right] M_{h_0}^2 \\
& + M_{A_0}^2 \left[(-2M_{h_0}^2 + 2M_{H^\pm}^2 - M_W^2)M_{h_0}^2 + M_W^2(M_{H^\pm}^2 - 2M_W^2) \right] \\
& \left. + M_W^2 \left[3M_{H^\pm}^2(-M_{H^\pm}^2 + M_W^2 + k_{12} + k_{13}) + 2M_W^2(k_{12} + k_{13}) \right] \right\} \times \\
& \times D_1[M_{h_0}^2, M_{h_0}^2, 0, M_{A_0}^2; k_{12}, k_{23}; H^\pm, W, W, W], \tag{43}
\end{aligned}$$

$$\begin{aligned}
\frac{G_4}{M_W^2} = & \left\{ 2(M_{A_0}^2 - 4M_{h_0}^2 + 3M_{H^\pm}^2 - 3M_W^2)D_{00} + 2(M_{A_0}^2 - M_{H^\pm}^2 - M_W^2)(M_{A_0}^2 D_2 + k_{12} D_3) \right. \\
& + 2(M_{A_0}^2 - M_{H^\pm}^2 - M_W^2)(2M_{A_0}^2 + M_{h_0}^2 + M_{H^\pm}^2 - M_W^2 - k_{12} - k_{13})D_0 \\
& + \left[(-M_{A_0}^2 - 6M_{h_0}^2 + 5M_{H^\pm}^2 - 8M_W^2 + k_{12} + 2k_{13})M_{A_0}^2 \right. \\
& \left. + M_{H^\pm}^2 k_{12} + 2M_W^2 k_{13} - 2M_{h_0}^2(M_W^2 - M_{h_0}^2 + k_{12} + k_{13}) \right] D_{11} \\
& + \left[(2M_{h_0}^2 + 2M_{H^\pm}^2 - 7M_W^2 - 2k_{12} + 2k_{13})M_{h_0}^2 + M_{H^\pm}^2 k_{12} \right. \\
& \left. + M_{A_0}^2(-6M_{h_0}^2 + 2M_{H^\pm}^2 - 3M_W^2 + k_{12}) + (3M_W^2 - 2M_{H^\pm}^2)k_{13} \right] D_{13} \\
& + \left[(-M_{A_0}^2 - 10M_{h_0}^2 + 5M_{H^\pm}^2 - 8M_W^2 + 2k_{12} + 2k_{13})M_{A_0}^2 \right. \\
& \left. + M_{h_0}^2(4M_{h_0}^2 + 2M_{H^\pm}^2 - 9M_W^2) \right. \\
& \left. - (2M_{H^\pm}^2 - 5M_W^2)(k_{12} + k_{13}) \right] D_{12} \left. \right\} [M_{A_0}^2, M_{h_0}^2, 0, M_{h_0}^2; k_{23}, k_{13}; H^\pm, W, W, W] \\
& + \frac{1}{M_W^2} \left\{ \left[(-2M_{h_0}^2 + 2M_{H^\pm}^2 - 3M_W^2)M_{h_0}^2 + M_W^2(2M_{A_0}^2 + 3M_{H^\pm}^2 - k_{12} + k_{13}) \right] M_{A_0}^2 \right. \\
& + \left[M_W^2(M_W^2 - 2k_{12} - 4k_{13}) - M_{H^\pm}^2(M_{H^\pm}^2 + k_{12} + 3k_{13}) \right] M_W^2 \\
& \left. + \left[2M_{h_0}^2(M_{H^\pm}^2 - M_W^2) + 2M_W^2(3M_W^2 + k_{12} + k_{13}) + M_{H^\pm}^2(M_W^2 - 2M_{H^\pm}^2) \right] M_{h_0}^2 \right\} \times \\
& \times D_1[M_{A_0}^2, M_{h_0}^2, 0, M_{h_0}^2; k_{23}, k_{13}; H^\pm, W, W, W], \tag{44}
\end{aligned}$$

$$\begin{aligned}
\frac{G_5}{M_W^2} = & \left\{ 4(M_{A_0}^2 - M_{h_0}^2 - M_W^2)D_{00} - \left[(M_{H^\pm}^2 - 5M_{h_0}^2 + 4M_W^2 + k_{12} - k_{13})M_{h_0}^2 \right. \right. \\
& + (M_{H^\pm}^2 + 2M_W^2)k_{12} + M_{A_0}^2(5M_{h_0}^2 - M_{H^\pm}^2 - 2k_{12}) + M_{H^\pm}^2k_{13} \left. \right] D_1 \\
& - \left[2k_{12}(M_{h_0}^2 + 2M_W^2) + M_{A_0}^2(M_{h_0}^2 - M_{H^\pm}^2 + 2M_W^2 - 2k_{12}) \right] D_{22} \\
& + \left[(M_{h_0}^2 + 3M_{H^\pm}^2 - 6M_W^2 - k_{12} + k_{13})M_{h_0}^2 - M_{H^\pm}^2k_{12} \right. \\
& + M_{A_0}^2(-5M_{h_0}^2 + M_{H^\pm}^2 - 2M_W^2 + 2k_{12}) + (2M_W^2 - M_{H^\pm}^2)k_{13} \left. \right] (D_{12} + D_{13}) \\
& - \left[(2M_W^2 - M_{h_0}^2 - M_{H^\pm}^2 + 3k_{12} + k_{13})M_{h_0}^2 + (M_{H^\pm}^2 + 4M_W^2)k_{12} \right. \\
& + (M_{H^\pm}^2 - 2M_W^2)k_{13} + M_{A_0}^2(5M_{h_0}^2 - 3M_{H^\pm}^2 + 8M_W^2 - 4k_{12} - 2k_{13}) \left. \right] D_{23} \\
& - \left[(-M_{h_0}^2 + 4M_{A_0}^2 - M_{H^\pm}^2 + 2M_W^2 + k_{12} + k_{13})M_{h_0}^2 + M_{H^\pm}^2k_{12} + (M_{H^\pm}^2 - 2M_W^2)k_{13} \right. \\
& \left. - 2M_{A_0}^2(M_{H^\pm}^2 - 3M_W^2 + k_{12} + k_{13}) \right] D_{33} \left. \right\} [M_{h_0}^2, M_{h_0}^2, 0, M_{A_0}^2; k_{12}, k_{13}; H^\pm, W, W, W] \\
& + \frac{1}{M_W^2} \left\{ M_{h_0}^4(2M_{H^\pm}^2 + M_W^2) - \left[2M_{H^\pm}^4 + M_W^2(M_W^2 + k_{12}) \right] M_{h_0}^2 \right. \\
& + M_W^2 \left[M_{H^\pm}^2(-5M_{H^\pm}^2 + 5M_W^2 + 3k_{12}) + 2M_W^2k_{12} \right] \\
& \left. + M_{A_0}^2 \left[(-2M_{h_0}^2 + 2M_{H^\pm}^2 + 3M_W^2)M_{h_0}^2 + M_W^2(M_{H^\pm}^2 - 2k_{12}) \right] \right\} \times \\
& \times D_0[M_{h_0}^2, M_{h_0}^2, 0, M_{A_0}^2; k_{12}, k_{13}; H^\pm, W, W, W] \\
& + \frac{1}{M_W^2} \left\{ 2M_{h_0}^4(M_{H^\pm}^2 - M_W^2) \right. \\
& + \left[M_{H^\pm}^2(3M_W^2 - 2M_{H^\pm}^2) + M_W^2(3M_W^2 + 2k_{12} + k_{13}) \right] M_{h_0}^2 \\
& + M_W^2 \left[(-3M_{H^\pm}^2 + 3M_W^2 - 2k_{12} - 3k_{13})M_{H^\pm}^2 - 2M_W^2(k_{12} + k_{13}) \right] \\
& \left. + M_{A_0}^2 \left[(-2M_{h_0}^2 + 2M_{H^\pm}^2 - 3M_W^2)M_{h_0}^2 + M_W^2(5M_{H^\pm}^2 - 2M_W^2 + 2k_{13}) \right] \right\} \times \\
& \times D_3[M_{h_0}^2, M_{h_0}^2, 0, M_{A_0}^2; k_{12}, k_{13}; H^\pm, W, W, W] \\
& + \frac{1}{M_W^2} \left\{ \left[M_{h_0}^2(2M_{H^\pm}^2 - 5M_W^2) + 2M_{H^\pm}^2(2M_W^2 - M_{H^\pm}^2) \right. \right. \\
& + M_W^2(5M_W^2 + 3k_{12} + 4k_{13}) \left. \right] M_{h_0}^2 \\
& - 2M_{A_0}^2 \left[(M_{h_0}^2 + M_W^2 - M_{H^\pm}^2)M_{h_0}^2 - M_W^2(3M_{H^\pm}^2 + M_W^2) \right] \\
& \left. + M_W^2 \left[M_{H^\pm}^2(-3M_{H^\pm}^2 + 3M_W^2 - 3k_{12} - 4k_{13}) - 2M_W^2(3k_{12} + 2k_{13}) \right] \right\} \times \\
& \times D_2[M_{h_0}^2, M_{h_0}^2, 0, M_{A_0}^2; k_{12}, k_{13}; H^\pm, W, W, W].
\end{aligned} \tag{45}$$

We next to decompose the one-loop form factors $F_{(SS,W)}^{(\text{Box})}$ as follows:

$$\begin{aligned} \frac{F_{(SS,W)}^{(\text{Box})}}{k_1 \cdot k_3} &= -\frac{e^2}{8\pi^2} \left(\frac{g_{h_0 h_0 H^\pm G^\mp}}{M_W s_W} \right) \cdot H_0 \\ &\quad - \frac{ie^3}{16\pi^2} \left(\frac{c_{\beta-\alpha}}{M_W^2 s_{2W}} \right) g_{h_0 H^\pm H^\mp} \cdot \sum_{i=1}^3 H_i \\ &\quad - \frac{e^4}{16\pi^2} \left(\frac{s_{2(\beta-\alpha)}}{M_W^3 s_{2W}^2 c_W} \right) \cdot \sum_{i=4}^6 H_i. \end{aligned} \quad (46)$$

Both general couplings in the above equation are obtained as in Eqs. (37) and (39). All coefficient factors H_i for $i = 0, 1, \dots, 6$ given in the above equation, are listed in terms of PV-functions as follows:

$$\frac{H_0}{M_W^2} = \frac{(M_{A_0}^2 - M_{H^\pm}^2)}{M_W^2} C_2[0, k_{12}, M_{A_0}^2; H^\pm, H^\pm, W], \quad (47)$$

$$\begin{aligned} \frac{H_1}{M_W^2} &= [C_2 - C_1 - C_0][M_{h_0}^2, k_{12}, M_{h_0}^2; H^\pm, H^\pm, W] \\ &\quad + [C_2 + C_1 - C_0][M_{h_0}^2, k_{23}, M_{A_0}^2; H^\pm, H^\pm, W] - 2C_0[M_{h_0}^2, 0, k_{23}; H^\pm, W, W] \\ &\quad + [C_2 - C_0][M_{h_0}^2, k_{13}, M_{A_0}^2; H^\pm, H^\pm, W] - 4C_0[M_{h_0}^2, 0, k_{13}; H^\pm, W, W], \end{aligned} \quad (48)$$

$$\begin{aligned} \frac{H_2}{M_W^2} &= \left[4D_{00} + (M_{A_0}^2 - M_{h_0}^2 + k_{12} - k_{13})(D_{12} + D_{13}) + (M_{A_0}^2 - 5M_{h_0}^2 + k_{12} - k_{13})D_1 \right. \\ &\quad \left. + (3M_{A_0}^2 - M_{h_0}^2 + 3k_{12} + k_{13})D_{23} + (2M_{A_0}^2 - M_{h_0}^2 + k_{12} + k_{13})D_{33} \right. \\ &\quad \left. + (M_{A_0}^2 + 2k_{12})D_{22} \right] [M_{h_0}^2, M_{h_0}^2, 0, M_{A_0}^2; k_{12}, k_{13}; H^\pm, H^\pm, W, W] \\ &\quad + \frac{1}{M_W^2} \left[M_W^2(-M_{A_0}^2 - M_{h_0}^2 - 2M_{H^\pm}^2 + k_{12}) + 2(M_{A_0}^2 - M_{H^\pm}^2)(M_{h_0}^2 - M_{H^\pm}^2) \right] \times \\ &\quad \times D_0[M_{h_0}^2, M_{h_0}^2, 0, M_{A_0}^2; k_{12}, k_{13}; H^\pm, H^\pm, W, W] \\ &\quad + \left[M_W^2(4M_{A_0}^2 + 5M_{h_0}^2 - 2M_{H^\pm}^2 - 3k_{12} - 4k_{13}) + 2(M_{A_0}^2 - M_{H^\pm}^2)(M_{h_0}^2 - M_{H^\pm}^2) \right] \times \\ &\quad \times D_2[M_{h_0}^2, M_{h_0}^2, 0, M_{A_0}^2; k_{12}, k_{13}; H^\pm, H^\pm, W, W] \\ &\quad + \frac{1}{M_W^2} \left[M_W^2(3M_{A_0}^2 + 2M_{h_0}^2 - 2M_{H^\pm}^2 - 2k_{12} - k_{13}) + 2(M_{A_0}^2 - M_{H^\pm}^2)(M_{h_0}^2 - M_{H^\pm}^2) \right] \times \\ &\quad \times D_3[M_{h_0}^2, M_{h_0}^2, 0, M_{A_0}^2; k_{12}, k_{13}; H^\pm, H^\pm, W, W]. \end{aligned} \quad (49)$$

The further coefficient factors are given by

$$\begin{aligned}
\frac{H_3}{M_W^2} = & \left[2D_{00} - (3M_{h_0}^2 - 2k_{12} - k_{13})D_{11} + (M_{A_0}^2 - 3M_{h_0}^2 + 4k_{12} + k_{13})D_{12} \right. \\
& + (3M_{A_0}^2 - 2M_{h_0}^2 + 2k_{12})D_{13} + (3M_{A_0}^2 + M_{h_0}^2 - k_{13})D_{33} \\
& + (4M_{A_0}^2 + M_{h_0}^2 + 2k_{12} - k_{13})D_{23} \\
& \left. + (M_{A_0}^2 + 2k_{12})D_{22} \right] [M_{h_0}^2, M_{h_0}^2, 0, M_{A_0}^2; k_{12}, k_{23}; H^\pm, H^\pm, W, W] \\
& + \frac{1}{M_W^2} \left[M_{A_0}^2 (2M_{h_0}^2 - 2M_{H^\pm}^2 + M_W^2) - M_{h_0}^2 (2M_{H^\pm}^2 + M_W^2) \right. \\
& \left. + 2M_{H^\pm}^2 (M_{H^\pm}^2 - M_W^2) - M_W^2 k_{12} \right] D_0 [M_{h_0}^2, M_{h_0}^2, 0, M_{A_0}^2; k_{12}, k_{23}; H^\pm, H^\pm, W, W] \\
& + \frac{1}{M_W^2} \left[M_W^2 (-M_{A_0}^2 - 8M_{h_0}^2 - 2M_{H^\pm}^2 + 3k_{12} + 3k_{13}) \right. \\
& \left. + 2(M_{A_0}^2 - M_{H^\pm}^2)(M_{h_0}^2 - M_{H^\pm}^2) \right] D_1 [M_{h_0}^2, M_{h_0}^2, 0, M_{A_0}^2; k_{12}, k_{23}; H^\pm, H^\pm, W, W] \\
& + \frac{1}{M_W^2} \left[M_W^2 (-2M_{A_0}^2 - 2M_{H^\pm}^2 - 3M_{h_0}^2 + 3k_{12} + 4k_{13}) \right. \\
& \left. + 2(M_{A_0}^2 - M_{H^\pm}^2)(M_{h_0}^2 - M_{H^\pm}^2) \right] D_2 [M_{h_0}^2, M_{h_0}^2, 0, M_{A_0}^2; k_{12}, k_{23}; H^\pm, H^\pm, W, W] \\
& + \left[2(M_{A_0}^2 - M_{H^\pm}^2)(M_{h_0}^2 - M_{H^\pm}^2) - M_W^2 (2M_{H^\pm}^2 - k_{12} - k_{13}) \right] \times \\
& \times D_3 [M_{h_0}^2, M_{h_0}^2, 0, M_{A_0}^2; k_{12}, k_{23}; H^\pm, H^\pm, W, W], \tag{50}
\end{aligned}$$

$$\begin{aligned}
\frac{H_4}{M_W^2} = & \frac{1}{M_W^2} \left[M_{A_0}^2 (M_{h_0}^2 - M_{H^\pm}^2 - M_W^2) - 2M_W^4 - M_{h_0}^2 (M_{H^\pm}^2 + M_W^2) \right. \\
& \left. + M_{H^\pm}^2 (M_{H^\pm}^2 + 2M_W^2) \right] C_2 [0, k_{13}, M_{h_0}^2; H^\pm, H^\pm, W], \tag{51}
\end{aligned}$$

$$\begin{aligned}
\frac{H_5}{M_W^2} = & \left\{ (2M_{A_0}^2 + 2M_{h_0}^2 - 4M_{H^\pm}^2 + 8M_W^2)D_{00} - \left[M_{A_0}^2 (M_{h_0}^2 - 2M_{H^\pm}^2 + 3M_W^2 + k_{13}) \right. \right. \\
& + M_{h_0}^2 (M_{h_0}^2 - M_W^2 - 2k_{12} - k_{13}) + (2M_{H^\pm}^2 - 3M_W^2)k_{12} + M_W^2 k_{13} \left. \right] (D_{12} + D_{13}) \\
& + \left[M_{A_0}^2 (M_{h_0}^2 - M_{H^\pm}^2 + 2M_W^2 + k_{12}) + k_{12} (2M_{h_0}^2 - 3M_{H^\pm}^2 + 5M_W^2) \right] D_{22} \\
& + \left[M_{A_0}^2 (3M_{h_0}^2 - M_{H^\pm}^2 + 2M_W^2 + k_{12}) + M_{h_0}^2 (-3M_{h_0}^2 + M_{H^\pm}^2 + 4k_{12} + k_{13}) \right. \\
& + (8M_W^2 - 5M_{H^\pm}^2)k_{12} + (2M_W^2 - M_{H^\pm}^2)k_{13} \left. \right] D_{23} \\
& + \left[M_{h_0}^2 (2M_{A_0}^2 - 3M_{h_0}^2 + M_{H^\pm}^2 + 2k_{12} + k_{13}) + (3M_W^2 - 2M_{H^\pm}^2)k_{12} \right. \\
& + (2M_W^2 - M_{H^\pm}^2)k_{13} \left. \right] D_{33} \left. \right\} [0, M_{A_0}^2, M_{h_0}^2, M_{h_0}^2; k_{12}, k_{13}; H^\pm, H^\pm, W, W] \\
& + \frac{1}{M_W^2} \left\{ M_{A_0}^2 \left[M_{h_0}^2 (M_{h_0}^2 - M_{H^\pm}^2 - 2M_W^2) + M_W^2 (M_{H^\pm}^2 - M_W^2 + 2k_{12}) \right] \right. \\
& + M_{h_0}^2 \left[M_{H^\pm}^2 (M_{H^\pm}^2 + 3M_W^2) - M_{h_0}^2 (M_{H^\pm}^2 + 2M_W^2) + M_W^2 (M_W^2 + 2k_{12} + 2k_{13}) \right] \\
& + M_W^2 \left[2M_{H^\pm}^2 (M_W^2 - 2k_{12} - k_{13}) + M_W^2 (-2M_W^2 + k_{12} - 2k_{13}) \right] \left. \right\} \times \\
& \times (D_2 + D_3) [0, M_{A_0}^2, M_{h_0}^2, M_{h_0}^2; k_{12}, k_{13}; H^\pm, H^\pm, W, W], \tag{52}
\end{aligned}$$

$$\begin{aligned}
\frac{H_6}{M_W^2} = & \left\{ (4M_{h_0}^2 - 4M_{H^\pm}^2 + 6M_W^2)D_{00} - \left[M_{A_0}^2 (M_{A_0}^2 + 2M_{h_0}^2 - 2M_{H^\pm}^2 + 4M_W^2 - k_{12} - k_{13}) \right. \right. \\
& + M_{h_0}^2 (-M_{h_0}^2 + M_W^2 - k_{12} + k_{13}) + (2M_{H^\pm}^2 - 4M_W^2)k_{12} - M_W^2 k_{13} \left. \right] D_{12} \\
& + \left[M_{A_0}^2 (M_{h_0}^2 - M_{H^\pm}^2 + 2M_W^2 + k_{12}) + k_{12} (2M_{h_0}^2 - 3M_{H^\pm}^2 + 5M_W^2) \right] D_{22} \\
& + \left[M_{A_0}^2 (3M_{h_0}^2 - M_{H^\pm}^2 + 2M_W^2) \right. \\
& - M_{h_0}^2 (M_{h_0}^2 + M_{H^\pm}^2 - 4M_W^2 - k_{12} + k_{13}) - M_W^2 k_{13} \\
& + (M_{H^\pm}^2 - M_W^2)(k_{13} - k_{12}) \left. \right] D_{23} \left. \right\} [0, M_{A_0}^2, M_{h_0}^2, M_{h_0}^2; k_{12}, k_{23}; H^\pm, H^\pm, W, W] \\
& + \frac{1}{M_W^2} \left\{ M_{A_0}^2 \left[M_{h_0}^2 (M_{h_0}^2 - M_{H^\pm}^2) - M_W^2 (M_{H^\pm}^2 + 3M_W^2 - 2k_{12}) \right] \right. \\
& + M_{h_0}^2 \left[M_{H^\pm}^2 (M_{H^\pm}^2 - M_W^2) - M_{h_0}^2 (M_{H^\pm}^2 - 2M_W^2) - M_W^2 (3M_W^2 + 2k_{13}) \right] \\
& + M_W^2 \left[2M_{H^\pm}^2 (M_W^2 - k_{12} + k_{13}) - M_W^2 (2M_W^2 - 3k_{12} - 2k_{13}) \right] \left. \right\} \times \\
& \times D_2 [0, M_{A_0}^2, M_{h_0}^2, M_{h_0}^2; k_{12}, k_{23}; H^\pm, H^\pm, W, W]. \tag{53}
\end{aligned}$$

Finally, we consider the last form factors $F_{(SSS,W)}^{(\text{Box})}$ which are shown as follows:

$$\frac{F_{(SSS,W)}^{(\text{Box})}}{k_1 \cdot k_3} = \frac{ie^3}{16\pi^2} \left(\frac{c_{\beta-\alpha}}{M_W^2 s_W^2} \right) \cdot \sum_{i=0}^5 K_i. \tag{54}$$

In this equation, all factors K_i are listed in terms of PV-functions as follows:

$$\frac{K_0}{M_W^2} = -(C_0 + C_1 + C_2)[M_{h_0}^2, 0, k_{13}; H^\pm, H^\pm, H^\pm], \quad (55)$$

$$\begin{aligned} \frac{K_1}{M_W^2} = & - \left[2D_{00} - (M_{A_0}^2 + 3M_{h_0}^2 - k_{13})D_{23} - (M_{A_0}^2 + 3M_{h_0}^2 - k_{13})D_{13} \right. \\ & - (3M_{h_0}^2 - 2k_{12} - k_{13})D_{11} + (2M_{A_0}^2 - 5M_{h_0}^2 + 2k_{12} + k_{13})D_{12} + 2(M_{A_0}^2 - M_{h_0}^2)D_{22} \\ & \left. - (M_{A_0}^2 + 3M_{h_0}^2 - k_{13})D_3 \right] [M_{h_0}^2, 0, M_{A_0}^2, M_{h_0}^2; k_{13}, k_{12}; H^\pm, H^\pm, H^\pm, W] \\ & + \left[M_{A_0}^2(M_{h_0}^2 - M_{H^\pm}^2) - M_W^2(M_{A_0}^2 - M_{h_0}^2 + M_W^2 - k_{13}) + M_{H^\pm}^2(M_{H^\pm}^2 - M_{h_0}^2) \right] \times \\ & \times D_0[M_{h_0}^2, 0, M_{A_0}^2, M_{h_0}^2; k_{13}, k_{12}; H^\pm, H^\pm, H^\pm, W] \\ & + \left[M_{A_0}^2(M_{h_0}^2 - M_{H^\pm}^2) - M_W^2(M_{A_0}^2 - 4M_{h_0}^2 + M_W^2 + 2k_{12}) + M_{H^\pm}^2(M_{H^\pm}^2 - M_{h_0}^2) \right] \times \\ & \times D_1[M_{h_0}^2, 0, M_{A_0}^2, M_{h_0}^2; k_{13}, k_{12}; H^\pm, H^\pm, H^\pm, W] \\ & + \left[M_{A_0}^2(M_{h_0}^2 - M_{H^\pm}^2) - M_W^2(3M_{A_0}^2 - 3M_{h_0}^2 + M_W^2 - k_{13}) + M_{H^\pm}^2(M_{H^\pm}^2 - M_{h_0}^2) \right] \times \\ & \times D_2[M_{h_0}^2, 0, M_{A_0}^2, M_{h_0}^2; k_{13}, k_{12}; H^\pm, H^\pm, H^\pm, W], \quad (56) \end{aligned}$$

$$\begin{aligned} \frac{K_2}{M_W^2} = & \left[-4D_{00} + (M_{A_0}^2 - M_{h_0}^2 + k_{12} - k_{13})D_{13} - (M_{h_0}^2 + k_{12} + k_{13})D_{33} \right. \\ & \left. + 2(M_{A_0}^2 - M_{h_0}^2)D_{23} \right] [M_{h_0}^2, 0, M_{A_0}^2, M_{h_0}^2; k_{23}, k_{12}; H^\pm, H^\pm, H^\pm, W], \quad (57) \end{aligned}$$

$$\begin{aligned} \frac{K_3}{M_W^2} = & - \left[4D_{00} - 2(M_{A_0}^2 - M_{h_0}^2)D_{23} + (M_{h_0}^2 + k_{12} + k_{13})D_{33} \right. \\ & \left. - (M_{A_0}^2 - M_{h_0}^2 - k_{12} + k_{13})D_{13} \right] [0, M_{h_0}^2, M_{A_0}^2, M_{h_0}^2; k_{23}, k_{13}; H^\pm, H^\pm, H^\pm, W] \\ & - \frac{1}{M_W^2} \left[M_{A_0}^2(M_{h_0}^2 - M_{H^\pm}^2) - M_W^2(k_{12} + k_{13} - 3M_{h_0}^2 + M_W^2) + M_{H^\pm}^2(M_{H^\pm}^2 - M_{h_0}^2) \right] \times \\ & \times D_3[0, M_{h_0}^2, M_{A_0}^2, M_{h_0}^2; k_{23}, k_{13}; H^\pm, H^\pm, H^\pm, W], \quad (58) \end{aligned}$$

$$\begin{aligned}
\frac{K_4}{M_W^2} = & - \left[(k_{12} - 2M_{h_0}^2)D_{11} + (M_{A_0}^2 - 3M_{h_0}^2 + k_{12} - k_{13})D_{12} + (M_{A_0}^2 + M_{h_0}^2 - k_{13})D_{33} \right. \\
& + (M_{A_0}^2 - M_{h_0}^2 + k_{12} - k_{13})D_{13} + (M_{A_0}^2 - M_{h_0}^2 - k_{13})D_{22} \\
& \left. + 2(M_{A_0}^2 - k_{13})D_{23} \right] [M_{h_0}^2, 0, M_{h_0}^2, M_{A_0}^2; k_{13}, k_{23}; H^\pm, H^\pm, H^\pm, W] \\
& - \frac{1}{M_W^2} \left[M_{A_0}^2(M_{h_0}^2 - M_{H^\pm}^2) - M_W^2(M_{h_0}^2 + M_{H^\pm}^2 - k_{13}) + M_{H^\pm}^2(M_{H^\pm}^2 - M_{h_0}^2) \right] \times \\
& \times D_0[M_{h_0}^2, 0, M_{h_0}^2, M_{A_0}^2; k_{13}, k_{23}; H^\pm, H^\pm, H^\pm, W] \\
& - \frac{1}{M_W^2} \left[M_{A_0}^2(M_{h_0}^2 - M_{H^\pm}^2) - M_W^2(3M_{h_0}^2 + M_{H^\pm}^2 - k_{12} - k_{13}) + M_{H^\pm}^2(M_{H^\pm}^2 - M_{h_0}^2) \right] \times \\
& \times D_1[M_{h_0}^2, 0, M_{h_0}^2, M_{A_0}^2; k_{13}, k_{23}; H^\pm, H^\pm, H^\pm, W] \\
& - \frac{1}{M_W^2} \left[M_W^2(M_{A_0}^2 - 2M_{h_0}^2 - M_{H^\pm}^2) + M_{A_0}^2(M_{h_0}^2 - M_{H^\pm}^2) + M_{H^\pm}^2(M_{H^\pm}^2 - M_{h_0}^2) \right] \times \\
& \times D_2[M_{h_0}^2, 0, M_{h_0}^2, M_{A_0}^2; k_{13}, k_{23}; H^\pm, H^\pm, H^\pm, W] \\
& - \frac{1}{M_W^2} \left[M_{A_0}^2(M_{h_0}^2 - M_{H^\pm}^2) + M_W^2(M_{A_0}^2 - M_{H^\pm}^2) + M_{H^\pm}^2(M_{H^\pm}^2 - M_{h_0}^2) \right] \times \\
& \times D_3[M_{h_0}^2, 0, M_{h_0}^2, M_{A_0}^2; k_{13}, k_{23}; H^\pm, H^\pm, H^\pm, W], \tag{59}
\end{aligned}$$

$$\begin{aligned}
\frac{K_5}{M_W^2} = & - \frac{1}{M_W^2} \left[M_{A_0}^2(M_{h_0}^2 - M_{H^\pm}^2) - M_W^2(k_{12} + k_{13} - 3M_{h_0}^2 + M_W^2) + M_{H^\pm}^2(M_{H^\pm}^2 - M_{h_0}^2) \right] \times \\
& \times D_3[M_{h_0}^2, 0, M_{A_0}^2, M_{h_0}^2; k_{23}, k_{12}; H^\pm, H^\pm, H^\pm, W]. \tag{60}
\end{aligned}$$

After collecting all the necessary form factors, we are going to check for the analytic results with verifying the UV -, IR -finiteness and Ward identity of one-loop amplitude. The numerical tests are shown in Tables 3, 4. From the data, we find that the numerical results of the tests are good stabilities. Having the corrseness one-loop form factors, the decay rates are then calculated as follows:

$$\Gamma_{A_0 \rightarrow h_0 h_0 \gamma} = \frac{1}{256\pi^3 M_{A_0}^3} \int_{k_{12}^{\min}}^{k_{12}^{\max}} dk_{12} \int_{k_{13}^{\min}}^{k_{13}^{\max}} dk_{13} \sum_{\text{pol.}} |\mathcal{M}_{A_0 \rightarrow h_0 h_0 \gamma}|^2 \tag{61}$$

where total amplitude is squared as

$$\sum_{\text{unpol.}} |\mathcal{M}_{A_0 \rightarrow h_0 h_0 \gamma}|^2 = \frac{4[k_{12}k_{13}k_{23} - M_{h_0}^2(M_{h_0}^2 - M_{A_0}^2)k_{12} - M_{A_0}^4 M_{h_0}^2]}{(M_{h_0}^2 - k_{13})^2 (M_{h_0}^2 - k_{23})^2} |F|^2. \tag{62}$$

The integration regions are in

$$k_{12}^{\min} = 4M_{h_0}^2, \quad k_{12}^{\max} = M_{A_0}^2, \tag{63}$$

$$k_{13}^{\max/\min} = \frac{1}{2} \left[M_{A_0}^2 + 2M_{h_0}^2 - k_{12} \pm (M_{A_0}^2 - k_{12}) \sqrt{1 - 4M_{h_0}^2/k_{12}} \right]. \tag{64}$$

In the next section, we are going to present phenomenological results for the decay process.

4. Phenomenological results

In phenomenological results, all physical input parameters in the SM are taken as same as in Ref. [17]. We are interested in the nearly alignment scenario, or taking $s_{\beta-\alpha} \rightarrow 1$ in this work. In particular, $s_{\beta-\alpha} = 0.95$ is selected for the following numerical analyses. While the mixing angle β is taken in the range of $2 \leq t_\beta < 8$. Furthermore, the soft-breaking scale for the Z_2 -symmetry is obtained as $M^2 = M_H^2$ in this work. For the decay widths of Z and the SM-like Higgs, we take their values as in Ref. [17]. In other cases, the decay widths of A_0^* (H^*) can be obtained as in Ref. [8] (in Ref. [54]), respectively.

In Table 2, the decay rates for $A_0 \rightarrow h_0 h_0 \gamma$ at several points in the parameter space of THDM are calculated. In the Table, we select $t_\beta = 3$, $M_{A_0} = M_{H^\pm}$. While the mass of CP-even Higgs is taken as $M_H = M_{A_0} - M_Z$. In this Table, the first column shows for the values of $500 \text{ GeV} \leq M_{A_0} \leq 1200 \text{ GeV}$. The numerical results for the decay rates of $\Gamma_{A_0 \rightarrow h_0 h_0 \gamma}$ are presented in the remaining columns which are corresponding to each type of THDM. The results show that the decay rates are proportional to M_{A_0} . The decay widths for this mode are very small for the mass regions $M_{A_0} \leq 500 \text{ GeV}$. They are order of $\mathcal{O}(1)$ KeV in the regions of $M_{A_0} \geq 800 \text{ GeV}$. We find that the results are lightly different from the distinct four types of the THDM. It is because the distinct four types of the THDM only come from all fermion exchanging in one-loop triangle diagrams with Z^* -poles (seen Eqs. (29), (33) for more detail). The contributions are proportional to the couplings $g_{h_0 f f}$ and give small contributions in comparison with other terms.

M_{A_0} [GeV]	$\Gamma_{A_0 \rightarrow h_0 h_0 \gamma}^{(I)}$ [KeV]	$\Gamma_{A_0 \rightarrow h_0 h_0 \gamma}^{(II)}$ [KeV]	$\Gamma_{A_0 \rightarrow h_0 h_0 \gamma}^{(X)}$ [KeV]	$\Gamma_{A_0 \rightarrow h_0 h_0 \gamma}^{(Y)}$ [KeV]
500	0.008772 ± 0.000009	0.008793 ± 0.000009	0.008773 ± 0.000009	0.008789 ± 0.000009
800	0.9325 ± 0.0009	0.9333 ± 0.0009	0.9323 ± 0.0009	0.9332 ± 0.0009
1000	5.378 ± 0.005	5.380 ± 0.005	5.378 ± 0.005	5.380 ± 0.005
1200	19.11 ± 0.02	19.11 ± 0.02	19.11 ± 0.02	19.11 ± 0.02

Table 2: The decay rates for the decay processes. In this Table, we chose $M_H = M_{A_0} - M_Z$, $s_{\beta-\alpha} = 0.95$ and $M_{H^\pm} = M_{A_0}$. Numerical results for the partial decay rates are generated by using the multidimensional numerical integration CUBA program [56].

In Fig. 5, the differential decay rates with respect to the invariant of Higgs-pair ($M_{h_0 h_0}$) in final state are scanned over the parameter t_β . We have already pointed out that the results are lightly different from considering the different types of the THDM. For this reason, we assume that there are no different results in the differential decay rates from varying the obvious types of the THDM. In the below plots, we take THDM type I as typical example. Additionally, we vary the mixing angle $2 \leq t_\beta \leq 8$. We also set $M_{A_0} = 800 \text{ GeV}$, $M_H = M_{A_0} - M_Z$, $s_{\beta-\alpha} = 0.95$ and $M_{H^\pm} = M_{A_0}$ correspondingly. The decay rates develop to the regions of $500 \text{ GeV} \leq M_{h_0 h_0} \leq 600 \text{ GeV}$ and they are then decreased to $M_{h_0 h_0} \sim 680 \text{ GeV}$. The decay rates are increased rapidly to the peak around $M_H \sim 710 \text{ GeV}$. The peaks are suppressed in the case of $4 \leq t_\beta \leq 6$, it may come from the cancellation of one-loop triangle and the mixing Z - γ with H^* -pole diagrams.

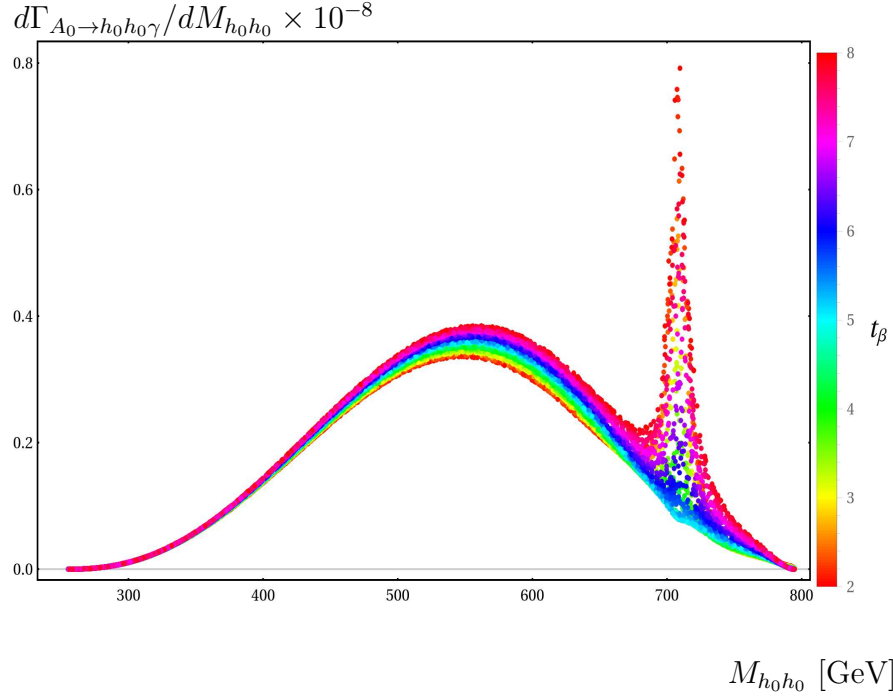


Figure 5: The differential decay rates with respect to the invariant of Higgs-pair ($M_{h_0 h_0}$) in final state are scanned over the parameter t_β . It is stress that we have used the label $d\Gamma_{A_0 \rightarrow h_0 h_0 \gamma} / dM_{h_0 h_0} \times 10^{-8}$. It means that numerical results shown in vertical axis must be multiplied by the factor 10^{-8} in this label.

In Fig. 6, the differential decay rates with respect to the invariant of Higgs-pair ($M_{h_0 h_0}$) in final state are scanned over the charged Higgs mass M_{H^\pm} (take THDM type I as a typical example). The input parameters are used as in the previous plot and fix the mixing angle $t_\beta = 3$. The results are generated with changing $200 \text{ GeV} \leq M_{H^\pm} \leq 1000 \text{ GeV}$. Overall, the differential decay rates develop to the regions $\sim 350 \text{ GeV} \leq M_{h_0 h_0} \leq \sim 730 \text{ GeV}$. They change slightly in the mentioned regions and decrease rapidly when $M_{h_0 h_0} \geq \sim 730 \text{ GeV}$. We also find small peaks of the differential decay rates around $M_H \sim 710 \text{ GeV}$.

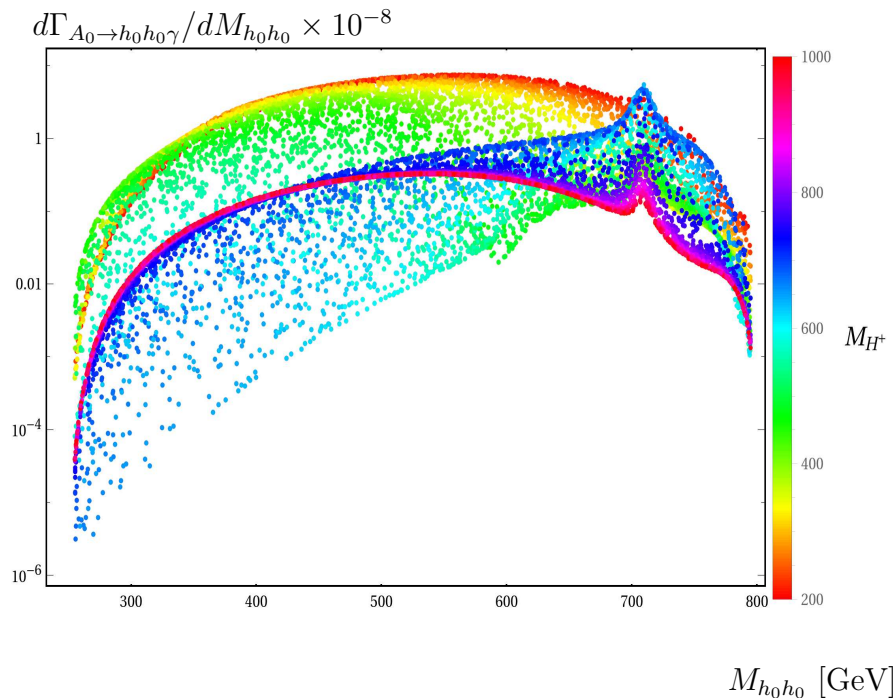


Figure 6: The differential decay rates with respect to the invariant of Higgs-pair ($M_{h_0 h_0}$) in final state are scanned over $M_{H^\pm}^2$.

5. Conclusions

For the first time, the analytic expressions for one-loop contributions to the rare decay amplitude $A_0 \rightarrow h_0 h_0 \gamma$ within the CP-conserving of the THDM have been introduced. They are written in term of scalar one-loop PV-functions in standard output of both the packages `LoopTools` and `Collier`. Numerical checks for the calculations such as the UV -, IR -finiteness, the Ward identity of one-loop amplitude are also performed in this article. In phenomenological results, the decay rates for $A_0 \rightarrow h_0 h_0 \gamma$ are examined at several allowed points in the parameter space of the THDM. Furthermore, the differential decay widths with respect to the invariant mass of Higgs-pair in final states are studied in the parameter space of the THDM.

Acknowledgment: This research is funded by Vietnam National Foundation for Science and Technology Development (NAFOSTED) under the grant number 103.01-2023.16.

Appendix A: Check for UV -finite of one-loop form factors

After collecting one-loop form factors, we are going to verify the analytic expressions by checking for UV -finite of one-loop form factors. Since there is no virtual photon exchanging in the loop. The results must be IR -finite. Moreover, we have no tree-level coupling of A_0 with $h_0 h_0 \gamma$. The decay channel starts at the contributions of one-loop Feynman diagrams. The results also must be UV -finite after summing all the contributed diagrams. In the course of dimensional regularization, one-loop Feynman integrals are regularised in the space-time dimension $d = 4 - 2\epsilon$ (for $\epsilon \rightarrow 0$ at final result). It is well-known that each one-loop diagram contains UV -divergent parts which are factorised as $C_{UV} = 1/\epsilon - \log(4\pi) + \gamma_E$ with Euler-Mascheroni constant $\gamma_E = 0.5772156 \dots$ (see Ref. [55] for more detail). The sum all diagrams for this process is being UV -finite. For the checks, we take the couplings of the THDM Type I as example. Other input parameters are listed as follows: $k_{12} = 500^2 \text{ GeV}^2$, $k_{13} = 300^2 \text{ GeV}^2$, $M_{A_0}^2 = 800^2 \text{ GeV}^2$,

$M_{H_0}^2 = 200^2 \text{ GeV}^2$, $M_{H^\pm}^2 = 250^2 \text{ GeV}^2$, $M^2 = 100^2 \text{ GeV}^2$, $t_\beta = 5$, and $s_{\beta-\alpha} = 0.95$. In the Table 3, we vary C_{UV} from 0 to 10^6 , one finds that the results are good stabilities over 14 digits in agreement. It shows that the one-loop form factors are UV -finite.

C_{UV}	$F(M_{A_0}^2, M_{h_0}^2; k_{12}, k_{13}, \dots)$
0	$3.1741294086792364 + 1.8029001762071715 i$
10^4	$3.1741294086792358 + 1.8029001762071712 i$
10^6	$3.1741294086792857 + 1.8029001762071708 i$

Table 3: In this Table, checks for the ultraviolet finiteness of one-loop form factors.

Appendix B: The Ward identity checks

For the decay process, we have a on-shell final photon. Subsequently, one-loop amplitude follows the Ward identity as explained in the section 3. In order to confirm the identity, two one-loop form factors F_1 and F_2 are collected independently. Their relation shown in Eq. (17) is then verified numerically. In the Table 4, the first column, we change the values of (k_{12}, k_{13}) . While the second and the last columns show the numerical values for two form factors F_1 and F_2 , respectively. For the tests, we use the input parameters as $M_{A_0}^2 = 800^2 \text{ GeV}^2$, $M_{H_0}^2 = 200^2 \text{ GeV}^2$, $M_{H^\pm}^2 = 250^2 \text{ GeV}^2$, $M^2 = 100^2 \text{ GeV}^2$, $t_\beta = 5$, and $s_{\beta-\alpha} = 0.95$. The results are shown in this Table is corresponding to the THDM type I taken as a typical example. The results are good stabilities over 12 digits. It confirms the identity numerically.

$(k_{12}, k_{13}) [\text{GeV}^2]$	$(k_1 \cdot k_3) \times F_1$	$-(k_2 \cdot k_3) \times F_2$
$(-100^2, -200^2)$	$+1.6380937118162464$ $+3.315236367886336 i$	$+1.6380937118162467$ $+3.315236367886336 i$
$(+100^2, -200^2)$	$+3.401930366245134$ $+3.3400883185466217 i$	$+3.401930366245136$ $+3.3400883185466217 i$
$(-100^2, +200^2)$	$+1.3135551033733244$ $-0.9792390439397629 i$	$+1.3135551033733248$ $-0.9792390439397629 i$
$(+100^2, +200^2)$	$+0.4278406932198653$ $-0.9572229486257442 i$	$+0.4278406932198655$ $-0.9572229486257442 i$

Table 4: In this Table, the numerical checks for the Ward identity of one-loop amplitude are performed with varying (k_{12}, k_{13}) .

References

- [1] G. Aad *et al.* [ATLAS], Phys. Lett. B **716** (2012), 1-29 doi:10.1016/j.physletb.2012.08.020 [arXiv:1207.7214 [hep-ex]].
- [2] S. Chatrchyan *et al.* [CMS], Phys. Lett. B **716** (2012), 30-61 doi:10.1016/j.physletb.2012.08.021 [arXiv:1207.7235 [hep-ex]].
- [3] R. Dermisek and J. F. Gunion, Phys. Rev. D **81** (2010), 055001 doi:10.1103/PhysRevD.81.055001 [arXiv:0911.2460 [hep-ph]].

- [4] G. Aad *et al.* [ATLAS], Phys. Lett. B **744** (2015), 163-183 doi:10.1016/j.physletb.2015.03.054 [[arXiv:1502.04478](#) [hep-ex]].
- [5] A. M. Sirunyan *et al.* [CMS], JHEP **08** (2020), 139 doi:10.1007/JHEP08(2020)139 [[arXiv:2005.08694](#) [hep-ex]].
- [6] G. Aad *et al.* [ATLAS], [[arXiv:2409.20381](#) [hep-ex]].
- [7] S. Chatrchyan *et al.* [CMS], Phys. Rev. Lett. **109** (2012), 121801 doi:10.1103/PhysRevLett.109.121801 [[arXiv:1206.6326](#) [hep-ex]].
- [8] M. Aiko, S. Kanemura and K. Sakurai, Nucl. Phys. B **986** (2023), 116047 doi:10.1016/j.nuclphysb.2022.116047 [[arXiv:2207.01032](#) [hep-ph]].
- [9] S. Kanemura, M. Kikuchi, K. Sakurai and K. Yagyu, Comput. Phys. Commun. **233** (2018), 134-144 doi:10.1016/j.cpc.2018.06.012 [[arXiv:1710.04603](#) [hep-ph]].
- [10] S. Kanemura, M. Kikuchi, K. Mawatari, K. Sakurai and K. Yagyu, Comput. Phys. Commun. **257** (2020), 107512 doi:10.1016/j.cpc.2020.107512 [[arXiv:1910.12769](#) [hep-ph]].
- [11] M. Aiko, S. Kanemura, M. Kikuchi, K. Sakurai and K. Yagyu, Comput. Phys. Commun. **301** (2024), 109231 doi:10.1016/j.cpc.2024.109231 [[arXiv:2311.15892](#) [hep-ph]].
- [12] A. G. Akeroyd, S. Alanazi and S. Moretti, [[arXiv:2408.08314](#) [hep-ph]].
- [13] A. G. Akeroyd, S. Alanazi and S. Moretti, J. Phys. G **50** (2023) no.9, 095001 doi:10.1088/1361-6471/ace3e1 [[arXiv:2301.00728](#) [hep-ph]].
- [14] C. Weber, H. Eberl and W. Majerotto, Phys. Rev. D **68** (2003), 093011 doi:10.1103/PhysRevD.68.093011 [[arXiv:hep-ph/0308146](#) [hep-ph]].
- [15] C. Weber, H. Eberl and W. Majerotto, Phys. Lett. B **572** (2003), 56-67 doi:10.1016/j.physletb.2003.07.083 [[arXiv:hep-ph/0305250](#) [hep-ph]].
- [16] F. A. Chishtie, V. Elias and T. G. Steele, J. Phys. G **26** (2000), 93-98 doi:10.1088/0954-3899/26/1/309 [[arXiv:hep-ph/9909374](#) [hep-ph]].
- [17] K. H. Phan, D. T. Tran and T. H. Nguyen, PTEP **2024** (2024) no.8, 083B02 doi:10.1093/ptep/ptae103 [[arXiv:2404.02417](#) [hep-ph]].
- [18] J. Yin, W. G. Ma, R. Y. Zhang and H. S. Hou, Phys. Rev. D **66** (2002), 095008 doi:10.1103/PhysRevD.66.095008.
- [19] K. Sasaki and T. Uematsu, Phys. Lett. B **781** (2018), 290-294 doi:10.1016/j.physletb.2018.04.005 [[arXiv:1712.00197](#) [hep-ph]].
- [20] T. Farris, J. F. Gunion, H. E. Logan and S. f. Su, Phys. Rev. D **68** (2003), 075006 doi:10.1103/PhysRevD.68.075006 [[arXiv:hep-ph/0302266](#) [hep-ph]].
- [21] A. Arhrib, Phys. Rev. D **67** (2003), 015003 doi:10.1103/PhysRevD.67.015003 [[arXiv:hep-ph/0207330](#) [hep-ph]].
- [22] A. G. Akeroyd, A. Arhrib and M. Capdequi Peyranere, Mod. Phys. Lett. A **14** (1999), 2093-2108 [erratum: Mod. Phys. Lett. A **17** (2002), 373] doi:10.1142/S0217732399002157 [[arXiv:hep-ph/9907542](#) [hep-ph]].

- [23] A. G. Akeroyd, A. Arhrib and M. Capdequi Peyranere, Phys. Rev. D **64** (2001), 075007 [erratum: Phys. Rev. D **65** (2002), 099903] doi:10.1103/PhysRevD.65.099903 [[arXiv:hep-ph/0104243](#) [hep-ph]].
- [24] T. Hahn, Comput. Phys. Commun. **140** (2001), 418-431 doi:10.1016/S0010-4655(01)00290-9 [[arXiv:hep-ph/0012260](#) [hep-ph]].
- [25] T. Hahn and M. Perez-Victoria, Comput. Phys. Commun. **118** (1999), 153-165 doi:10.1016/S0010-4655(98)00173-8 [[arXiv:hep-ph/9807565](#) [hep-ph]].
- [26] A. Denner, S. Dittmaier and L. Hofer, Comput. Phys. Commun. **212** (2017), 220-238 doi:10.1016/j.cpc.2016.10.013 [[arXiv:1604.06792](#) [hep-ph]].
- [27] G. C. Branco, P. M. Ferreira, L. Lavoura, M. N. Rebelo, M. Sher and J. P. Silva, Phys. Rept. **516** (2012), 1-102 doi:10.1016/j.physrep.2012.02.002 [[arXiv:1106.0034](#) [hep-ph]].
- [28] M. Aoki, S. Kanemura, K. Tsumura and K. Yagyu, Phys. Rev. D **80** (2009), 015017 doi:10.1103/PhysRevD.80.015017 [[arXiv:0902.4665](#) [hep-ph]].
- [29] S. Nie and M. Sher, Phys. Lett. B **449** (1999), 89-92 doi:10.1016/S0370-2693(99)00019-2 [[arXiv:hep-ph/9811234](#) [hep-ph]].
- [30] S. Kanemura, T. Kasai and Y. Okada, Phys. Lett. B **471** (1999), 182-190 doi:10.1016/S0370-2693(99)01351-9 [[arXiv:hep-ph/9903289](#) [hep-ph]].
- [31] A. G. Akeroyd, A. Arhrib and E. M. Naimi, Phys. Lett. B **490** (2000), 119-124 doi:10.1016/S0370-2693(00)00962-X [[arXiv:hep-ph/0006035](#) [hep-ph]].
- [32] I. F. Ginzburg and I. P. Ivanov, Phys. Rev. D **72** (2005), 115010 doi:10.1103/PhysRevD.72.115010 [[arXiv:hep-ph/0508020](#) [hep-ph]].
- [33] S. Kanemura and K. Yagyu, Phys. Lett. B **751** (2015), 289-296 doi:10.1016/j.physletb.2015.10.047 [[arXiv:1509.06060](#) [hep-ph]].
- [34] L. Bian and N. Chen, JHEP **09** (2016), 069 doi:10.1007/JHEP09(2016)069 [[arXiv:1607.02703](#) [hep-ph]].
- [35] W. Xie, R. Benbrik, A. Habjia, S. Taj, B. Gong and Q. S. Yan, Phys. Rev. D **103** (2021) no.9, 095030 doi:10.1103/PhysRevD.103.095030 [[arXiv:1812.02597](#) [hep-ph]].
- [36] S. Kanemura, Y. Okada, H. Taniguchi and K. Tsumura, Phys. Lett. B **704** (2011), 303-307 doi:10.1016/j.physletb.2011.09.035 [[arXiv:1108.3297](#) [hep-ph]].
- [37] O. Eberhardt, A. P. Martínez and A. Pich, JHEP **05** (2021), 005 doi:10.1007/JHEP05(2021)005 [[arXiv:2012.09200](#) [hep-ph]].
- [38] L. Wang, J. M. Yang and Y. Zhang, Commun. Theor. Phys. **74** (2022) no.9, 097202 doi:10.1088/1572-9494/ac7fe9 [[arXiv:2203.07244](#) [hep-ph]].
- [39] A. Karan, V. Miralles and A. Pich, Phys. Rev. D **109** (2024) no.3, 3 doi:10.1103/PhysRevD.109.035012 [[arXiv:2307.15419](#) [hep-ph]].
- [40] D. W. Jung, Y. Heo and J. S. Lee, Phys. Rev. D **108** (2023) no.1, 015027 doi:10.1103/PhysRevD.108.015027 [[arXiv:2212.07620](#) [hep-ph]].

- [41] Y. H. Ahn, S. K. Kang and R. Ramos, Phys. Rev. D **106** (2022) no.5, 055038 doi:10.1103/PhysRevD.106.055038 [[arXiv:2204.06485](#) [hep-ph]].
- [42] A. Cici and H. Dag, [[arXiv:2403.10888](#) [hep-ph]].
- [43] S. Iguro, T. Kitahara, M. S. Lang and M. Takeuchi, Phys. Rev. D **108** (2023) no.11, 11 doi:10.1103/PhysRevD.108.115012 [[arXiv:2304.09887](#) [hep-ph]].
- [44] C. W. Chiang and K. Yagyu, Phys. Rev. D **87** (2013) no.3, 033003 doi:10.1103/PhysRevD.87.033003 [[arXiv:1207.1065](#) [hep-ph]].
- [45] R. Benbrik, M. Boukidi, M. Ouchemhou, L. Rahili and O. Tibssirte, Nucl. Phys. B **990** (2023), 116154 doi:10.1016/j.nuclphysb.2023.116154 [[arXiv:2211.12546](#) [hep-ph]].
- [46] J. Haller, A. Hoecker, R. Kogler, K. Mönig, T. Peiffer and J. Stelzer, Eur. Phys. J. C **78** (2018) no.8, 675 doi:10.1140/epjc/s10052-018-6131-3 [[arXiv:1803.01853](#) [hep-ph]].
- [47] J. M. Connell, P. Ferreira and H. E. Haber, Phys. Rev. D **108** (2023) no.5, 055031 doi:10.1103/PhysRevD.108.055031 [[arXiv:2302.13697](#) [hep-ph]].
- [48] P. Athron, A. Crivellin, T. E. Gonzalo, S. Iguro and C. Sierra, JHEP **11** (2024), 133 doi:10.1007/JHEP11(2024)133 [[arXiv:2410.10493](#) [hep-ph]].
- [49] M. Bohm, H. Spiesberger and W. Hollik, Fortsch. Phys. **34** (1986), 687-751 doi:10.1002/prop.19860341102
- [50] W. F. L. Hollik, Fortsch. Phys. **38** (1990), 165-260 doi:10.1002/prop.2190380302
- [51] K. I. Aoki, Z. Hioki, M. Konuma, R. Kawabe and T. Muta, Prog. Theor. Phys. Suppl. **73** (1982), 1-225 doi:10.1143/PTPS.73.1
- [52] S. Kanemura, M. Kikuchi, K. Sakurai and K. Yagyu, Phys. Rev. D **96** (2017) no.3, 035014 doi:10.1103/PhysRevD.96.035014 [[arXiv:1705.05399](#) [hep-ph]].
- [53] K. H. Phan, D. T. Tran and T. H. Nguyen, [[arXiv:2406.15749](#) [hep-ph]].
- [54] S. Kanemura, M. Kikuchi and K. Yagyu, Nucl. Phys. B **983** (2022), 115906 doi:10.1016/j.nuclphysb.2022.115906 [[arXiv:2203.08337](#) [hep-ph]].
- [55] A. Denner, Fortsch. Phys. **41** (1993), 307-420 doi:10.1002/prop.2190410402 [[arXiv:0709.1075](#) [hep-ph]].
- [56] T. Hahn, Comput. Phys. Commun. **168** (2005), 78-95 doi:10.1016/j.cpc.2005.01.010 [[arXiv:hep-ph/0404043](#) [hep-ph]].